

# PROPAGATION REVERSAL FOR BISTABLE DIFFERENTIAL EQUATIONS ON TREES

Hermen Jan Hupkes <sup>\*1</sup>, Mia Jukić <sup>†1</sup>, Petr Stehlík <sup>‡2</sup>, and Vladimír Švígler <sup>§2</sup>

<sup>1</sup>Mathematisch Instituut, Universiteit Leiden, P.O. Box 9512, 2300 RA Leiden, The Netherlands

<sup>2</sup>Department of Mathematics and NTIS, Faculty of Applied Sciences, University of West Bohemia, Univerzitní 8, 306 14 Plzeň, Czech Republic

June 13, 2022

## Abstract

We study traveling wave solutions to bistable differential equations on infinite  $k$ -ary trees. These graphs generalize the notion of classical square infinite lattices and our results complement those for bistable lattice equations on  $\mathbb{Z}$ . Using comparison principles and explicit lower and upper solutions, we show that wave-solutions are pinned for small diffusion parameters. Upon increasing the diffusion, the wave starts to travel with non-zero speed, in a direction that depends on the detuning parameter. However, once the diffusion is sufficiently strong, the wave propagates in a single direction up the tree irrespective of the detuning parameter. In particular, our results imply that changes to the diffusion parameter can lead to a reversal of the propagation direction.

**Keywords:** reaction-diffusion equations; lattice differential equations; travelling waves; propagation reversal; wave pinning; tree graphs.

**MSC 2010:** 34A33, 37L60, 39A12, 65M22

## 1 Introduction

In this paper we consider traveling wave solutions to the scalar bistable reaction-diffusion-advection lattice differential equation (LDE)

$$\begin{aligned} \dot{u}_i &= d(ku_{i+1} - (k+1)u_i + u_{i-1}) + g(u_i; a) \\ &= d(u_{i+1} - 2u_i + u_{i-1}) + d(k-1)(u_{i+1} - u_i) + g(u_i; a), \quad i \in \mathbb{Z}. \end{aligned} \quad (1.1)$$

Here  $d > 0$  is a diffusion parameter and the function  $g(u; a)$  is a bistable nonlinearity, such as the cubic

$$g(u; a) = u(1-u)(u-a), \quad a \in (0, 1). \quad (1.2)$$

As we explain below, the advection parameter  $k > 0$  can be interpreted as the branch factor of an infinite tree when it is integer valued.

We focus on the traveling front solutions of the form

$$u_i(t) = \Phi(i - ct), \quad \Phi(-\infty) = 0, \quad \Phi(\infty) = 1. \quad (1.3)$$

Our primary concern is how the diffusion strength  $d > 0$ , the branch factor  $k > 0$  and the detuning parameter  $a$  influence the sign of the wave-speed  $c$ . Fixing a value of  $k > 1$  for convenience, our main results can be summed up into the following three points (illustrated in Fig. 2(c)):

---

\*hhupkes@math.leidenuniv.nl

†m.jukic@math.leidenuniv.nl

‡pstehlik@kma.zcu.cz

§corresponding author, svigler@kma.zcu.cz

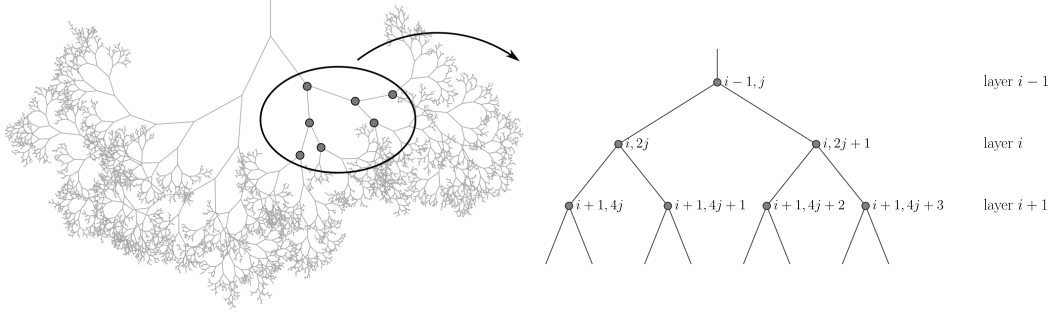


Figure 1: The infinite binary tree  $\mathcal{G} = \mathcal{T}_2$  with a sketch of the associated labelling scheme.

- (i) For any sufficiently small  $d > 0$ , wave pinning occurs in the sense that  $c = 0$  for a nonempty range of parameters  $a$  (Proposition 2.3).
- (ii) As we increase  $d$ , we have  $c < 0$  for all  $a \approx 0$  and  $c > 0$  for all  $a \approx 1$  (Theorem 2.6).
- (iii) For all  $a \in (0, 1)$  we have  $c < 0$  whenever  $d$  is sufficiently large (Theorem 2.5).

Consequently, these results show that for  $a \approx 1$  we can reverse the speed of the wave from  $c > 0$  to  $c < 0$  by increasing the diffusion parameter  $d$ ; see Fig. 2(c), Ex. 9.2 and Fig. 11 for illustration.

**Layer solutions on  $\mathcal{T}_k$**  Our primary motivation to study (1.1) is to further our understanding of reaction-diffusion equations on infinite  $k$ -ary trees, see Fig. 1. Such trees are (undirected) graphs  $\mathcal{T}_k = (V, E)$ ,  $k \in \mathbb{N}$  in which the set of vertices is given by  $V = \mathbb{Z} \times \mathbb{N}_0$  and the neighbourhood  $\mathcal{N}(i, j)$  of each node  $(i, j)$  consists of its parent node (in the  $(i - 1)$ -th layer) and  $k$  children (in the  $(i + 1)$ -th layer). We can explicitly characterize the set of edges  $E$  as

$$E = \{((i, j), (i + 1, kj + l)) : i \in \mathbb{Z}, j \in \mathbb{N}_0, l \in \{0, \dots, k - 1\}\}.$$

Note in particular that  $\mathcal{T}_1$  reduces to independent copies of  $\mathbb{Z}$  with nearest-neighbour edges.

Let us now consider the bistable reaction-diffusion system

$$\dot{u}_{i,j}(t) = d[\mathcal{L}_k u(t)]_{i,j} + g(u_{i,j}(t); a), \quad (i, j) \in V \quad (1.4)$$

posed on the tree  $\mathcal{T}_k$ , in which the operator

$$[\mathcal{L}_k u]_{i,j} = \sum_{(i', j') \in \mathcal{N}(i, j)} (u_{i', j'} - u_{i, j})$$

is commonly referred to as the graph Laplacian. We restrict our attention to so-called *layer solutions*, which satisfy the equality

$$u_{i,j}(t) = u_i(t)$$

for all  $(i, j) \in \mathbb{Z} \times \mathbb{N}_0$  and  $t \in \mathbb{R}$ . This substitution reduces the dynamics of (1.4) to that of (1.1). In particular, the traveling fronts (1.3) can be seen as layered invasion waves for the graph system (1.4). From this point of view it appears natural to take  $k \in \mathbb{N}$  in (1.1), but for our analysis it turns out to be worthwhile to also allow this parameter to be real.

In the following paragraphs we motivate our approach and briefly summarize the existing literature from the point of view of our results.

**Propagation through continuous media** Taking  $k = 1$ , LDE (1.1) can be considered as a spatially discrete approximation of the classical bistable partial differential equation

$$u_t(x, t) = \nu u_{xx}(x, t) + g(u(x, t); a), \quad x \in \mathbb{R}, \quad t > 0. \quad (1.5)$$

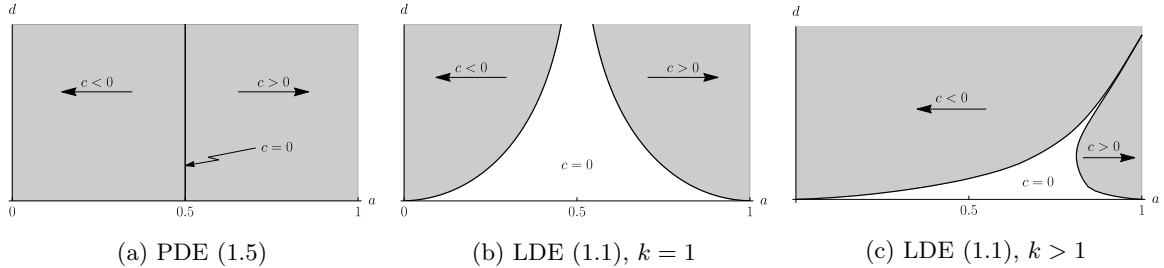


Figure 2: The dependence of the wave speed  $c$  on the detuning parameter  $a$  and the diffusion  $d$ . The left and middle panels show the well-known results for the PDE (1.5) and the LDE (1.1) with  $k = 1$ , i.e., (1.6). The right panel summarizes our results for the LDE (1.1) with  $k > 1$ .

Indeed, replacing the second derivative  $u_{xx}$  with the central difference scheme results in the system

$$\dot{u}_i(t) = d(u_{i+1}(t) - 2u_i(t) + u_{i-1}(t)) + g(u_i(t); a), \quad i \in \mathbb{Z}, \quad (1.6)$$

where  $u_i(t) \sim u(ih, t)$  and  $dh^2 = \nu$ . The bistable PDE (1.5) has been used to model the spread of genetic traits [2, 11], where it is often referred to as the *heterozygote inferior* case. It has also been proposed as a basic model for the propagation of electrical signals through unmyelinated nerve fibres, also known as the ‘reduced’ Fitzhugh-Nagumo equation [3, 21]. In general, (1.5) has played a prototypical role during the development of the theory of traveling waves that connect two stable states of the underlying nonlinearity [10].

Using phase-plane analysis [9], one can show that there exists a traveling wave solution

$$u(x, t) = \Phi(x - \sigma t), \quad \Phi(-\infty) = 0, \quad \Phi(+\infty) = 1$$

of (1.5) with

$$\text{sign}(\sigma) = -\text{sign} \left( \int_0^1 g(u; a) du \right).$$

This traveling wave satisfies the second order ODE

$$-\sigma \Phi'(\xi) = \nu \Phi''(\xi) + g(\Phi(\xi); a). \quad (1.7)$$

In the case of the cubic nonlinearity (1.2), there even exists an explicit solution formula for the speed  $\sigma$ , namely

$$\sigma = \sqrt{2\nu} \left( a - \frac{1}{2} \right). \quad (1.8)$$

From this equation it follows that  $\sigma = 0$  if and only if  $a = 1/2$ . The fact that we have  $\sigma = 0$  only at one value of the bistable parameter  $a$  is one of the fundamental differences between spatially continuous and discrete differential equations.

**Propagation through regular lattices** Lattice differential equations are a natural modelling tool when the underlying spatial domain has a discrete structure. Crystals [5], patchy landscapes [25, 26] and myelinated neurons [23] are all examples of such domains. One can find extensive lists of models and application areas in [13, 15].

Formally, equation (1.1) is a generalization of the classic bistable LDE (1.6), which has served as a prototypical example to study key phenomena like pinning and topological chaos. Indeed, it has attracted numerous studies, starting with the threshold propagation results in [3] and [4]. One of the first rigorous studies of propagation failure for (1.6) was conducted by Keener in [15], who established that  $c = 0$  can hold for a (non-trivial) interval of bistable parameters  $a$ . This is in stark contrast to the continuous bistable equation, where a slight change of the detuning parameter  $a$  suffices to cause standing waves to move. Keener in [15] applied the Moser theorem [20] to show

that for each  $a \in (0, 1)$  and sufficiently small diffusion  $0 < d \ll 1$  one can construct infinitely many horseshoe maps, with each of them giving rise to a stationary solution of (1.6) with values in  $[0, 1]$ . In addition, he constructed a larger region in the  $(a, d)$  plane where waves are pinned. On the other hand, he also established regions in the vicinity of  $a = 0$  and  $a = 1$  where fronts are guaranteed to propagate.

A general theory for the existence of traveling-wave solutions to a broad class of LDEs that includes (1.1) was developed by Mallet-Paret [18, 19], who performed a direct analysis of mixed functional difference equations (MFDEs) such as

$$-c\Phi'(\xi) = d(k\Phi(\xi + 1) - (k + 1)\Phi(\xi) + \Phi(\xi)) + g(\Phi(\xi); a), \quad (1.9)$$

which arises by substituting  $u_i(t) = \Phi(i - ct)$  into (1.1). His results guarantee that for each  $k > 0$ ,  $a \in (0, 1)$  and  $d > 0$  one can find a speed  $c \in \mathbb{R}$  and a profile  $\Phi : \mathbb{R} \rightarrow \mathbb{R}$  that satisfy (1.9). It should be remarked that the first existence result for  $k = 1$  was obtained by Zinner in [28] in the regime  $d \gg 0$ .

**Propagation through graphs** Dynamical systems on graphs serve naturally as a generalization of lattice equation where the interplay between finer graph properties and the dynamics can be investigated [24, 25, 26]. Trees represent an important class of graphs as they model processes on discrete media with regular branching structures [1]. Our paper is closely connected to a recent study by Kouvaris, Kori and Mikhailov [17], where approximation techniques are used to study propagation and pinning phenomena of waves on arbitrarily large, but finite  $k$ -ary trees. The bi-infinite trees that we consider in this paper (see Fig. 1) do not have a root vertex, in order to avoid the technical difficulties caused by adding boundaries to our spatial domain. However, due to the exponential convergence in the tails, we fully expect the traveling waves considered here to play an important organizing role for the dynamics on large but finite  $k$ -ary trees.

We expect that our results could also be relevant for more general graphs. For example, let us consider the Erdős-Rényi random graph  $ER_n(p)$  with  $n$  nodes, where the probability of two nodes being connected is given by  $p$  [8]. In the sparse regime where  $p = k/n$  for some fixed  $k > 0$ , one can show [7, 27] that the Erdős-Rényi random graph  $ER_n(k/n)$  converges locally in probability as  $n \rightarrow \infty$  to a Poisson branching process with mean offspring  $k$ . We can therefore consider  $k$ -ary trees as local approximations of large Erdős-Rényi random graphs. Consequently, wave propagation and pinning in random networks can be directly linked to the related phenomena on trees [16].

Similar ideas were explored very recently in [12] for the monostable Fisher-KPP equation on semi-infinite  $k$ -trees with one root. In this study, the authors consider initial conditions that are zero everywhere except at the root vertex and establish the existence of a critical diffusion parameter that separates (linear) spreading through the tree from extinction. Moreover, their numerical simulations suggest that this conclusion can be transferred in some sense to the dynamics of Erdős-Rényi random graphs.

**Comparison principle** Turning back to the original equation (1.1), we note that our main propagation results rely on the construction of appropriate sub- and super-solutions that push traveling waves to the left ( $c < 0$ ) or right ( $c > 0$ ), see Fig. 3. We use two different constructions, which yield qualitatively different conclusions.

Our first approach follows the outline from Keener [15] to construct smooth but ‘step-like’ sub-solutions. The simple nature of these functions results in a relatively tractable expression for the sub-solution residual, which we examine thoroughly in §5. Via this method we obtain a geometric description for a set  $\mathcal{D}^-$  in the  $(a, d)$ -plane where the wave speed is guaranteed to be negative. For the cubic nonlinearity, we are able to explicitly compute the boundary of  $\mathcal{D}^-$ , thus generalizing and completing the results from [15].

This approach has both advantages and disadvantages. On the one hand, the set  $\mathcal{D}^-$  obtained through this method is a priori bounded in  $d$ , unlike the actual region where  $c < 0$ . On the other hand, this method enables us to exploit a useful symmetry in the system that allows us to invert the sign of the wave speed. In particular, we also obtain a region  $\mathcal{D}^+$  close to  $a \approx 1$  where the

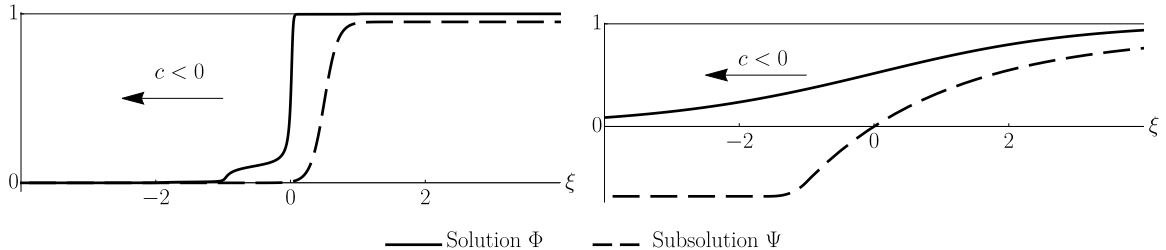


Figure 3: Subsolutions  $\Psi$  and numerically computed travelling waves  $\Phi$  with  $k = 5$  and  $a = 0.1933$  illustrating our two distinct approaches to construct subsolutions and predict the wavespeed sign. First, for small  $d$  we construct steep, almost step-like, subsolutions, see §5. The left panel shows an example with  $d = 0.00205$  and  $c \approx -0.0081$ . Next, for  $d \gg 0$ , we construct wide subsolutions  $\Psi$ , see §6. The right panel illustrates this approach with  $d = 0.4$  and  $c \approx -2.06$ .

wave speed is guaranteed to be strictly positive. Moreover, our numerical observations indicate that the lower boundaries of  $\mathcal{D}^-$  and  $\mathcal{D}^+$  are closely aligned with the edge of the pinning region. This result can be intuitively explained by the fact that traveling profiles close to the pinning regime are themselves almost step-like; see the left panel of Fig. 3. The steep sub-solutions therefore provide a good approximation of the actual wave-profiles.

Our second method relies on a more refined construction of sub-solutions. In particular, we build smooth and wide profiles that agree better with the actual wave-profile  $\Phi$  in the  $d \gg 0$  regime, see the right panel of Fig. 3. For every  $a \in (0, 1)$  we provide a value  $d^*(a)$  so that  $d > d^*$  implies  $c < 0$ , which shows that waves have a preferred  $a$ -independent direction of propagation. Together, these results allow us to paint a rather complete qualitative picture for general bistable nonlinearities.

**Propagation reversal** To gain some intuition for the diffusion-driven propagation reversal that occurs for  $a \approx 1$  and  $k > 1$ , let us substitute  $\Phi(\xi) = \psi(\xi h)$  into the travelling wave MFDE (1.9) to obtain

$$-ch\psi'(\xi) - (k-1)d[\psi(\xi+h) - \psi(\xi)] = d[\psi(\xi-h) + \psi(\xi+h) - 2\psi(\xi)] + g(\psi(\xi); a). \quad (1.10)$$

Taylor expanding around  $\psi(\xi)$  and sending  $h \rightarrow 0$  while keeping the quantities

$$\nu = \frac{1}{2}(k+1)dh^2, \quad \sigma = ch + (k-1)dh \quad (1.11)$$

fixed, this MFDE formally reduces to the travelling wave ODE (1.7). In particular, the wavespeed identity (1.8) for the cubic nonlinearity (1.2) now leads to the asymptotic prediction

$$c \sim \sqrt{(k+1)d} \left( a - \frac{1}{2} \right) - (k-1)d \quad (1.12)$$

for  $d \gg 1$ . For  $k > 1$  and  $a > \frac{1}{2}$  the right-hand side changes sign at the critical value

$$d_c(a, k) = \frac{(k+1)}{(k-1)^2} \left( a - \frac{1}{2} \right)^2 \quad (1.13)$$

which we expect to be increasingly accurate in the limit  $k \downarrow 1$ .

We believe that such a reversal mechanism for the direction of propagation has not been observed in the literature. Related studies have focussed on other mechanisms such as the scattering or combination of waves. For example, the numerical results in [22] indicate that the outcome of wave collisions for the PDE (1.5) depend on the properties of a class of unstable solutions called separators. The LDE (1.6) admits a class of generalized non-monotone (multichromatic) waves that can reverse their direction through intricate collision processes [14]. We note that a general theory to fully describe such collisions has not yet been developed.

**Organization** This paper is organised as follows. We set the stage and state our main results in §2. This section also includes explicit expressions for the propagation and pinning regions for the cubic nonlinearity. In §3 we summarize several consequences of the comparison principle that we use throughout the paper. We study the pinning region in §4 by establishing the existence of invariant intervals. In §5 we construct steep sub-solutions to establish the existence of the region  $\mathcal{D}^-$  in which the wave speed is negative. Exploiting a symmetry argument allows us to establish the equivalent results for positive speeds in the region  $\mathcal{D}^+$ . These two sections adapt the ideas from [15] to the more general setting considered in this work.

We proceed in §6 with the construction of wide sub-solutions that work well in the  $d \gg 0$  regime. Using the comparison principle we show that  $c < 0$  for all  $d \gg 0$ . Section §7 is dedicated to the cubic nonlinearity, as we provide explicit expressions for the boundaries of the sets  $\mathcal{D}^-$  and  $\mathcal{D}^+$ . In §8 we describe chaotic steady solutions to our initial LDE (1.1) by adapting the set-up from [15] and [20]. We conclude the paper with numerical examples to illustrate the reversal of propagation on  $k$ -ary trees in §9.

## 2 Main results

The main focus of our study is the reaction-diffusion-advection equation

$$\dot{u}_i(t) = d[\Delta_k u(t)]_i + g(u_i(t); a), \quad (2.1)$$

posed on the one dimensional lattice  $i \in \mathbb{Z}$ . The discrete diffusion-advection operator  $\Delta_k : \ell^\infty(\mathbb{Z}) \rightarrow \ell^\infty(\mathbb{Z})$  is defined by

$$\Delta_k u = u_{i-1} - (k+1)u_i + ku_{i+1}. \quad (2.2)$$

We require the nonlinearity  $g$  to satisfy the following standard bistability assumption.

(Hg) The map  $(u, a) \mapsto g(u; a)$  is  $C^1$ -smooth on  $\mathbb{R} \times [0, 1]$  and we have

$$\begin{aligned} g(0; a) &= g(a; a) = g(1; a) = 0, \\ g'(0; a) &< 0, \quad g'(1; a) < 0, \quad g'(a; a) > 0. \end{aligned}$$

In addition, the function  $g$  satisfies the inequalities

$$g(v; a) > 0 \text{ for } v \in (-\infty, 0) \cup (a, 1), \quad g(v; a) < 0 \text{ for } v \in (0, a) \cup (1, \infty).$$

Throughout this paper we write  $g'(v; a) = \partial_v g(v; a)$ . At times, we also need to impose the following additional assumptions on  $g$ .

(Hg1) For each  $a \in (0, 1)$  and  $v \in (0, 1)$  we have  $\partial_a g(v; a) < 0$ .

(Hg2) For each  $a \in [0, 1]$ , the nonlinearity  $g(\cdot; a)$  belongs to  $C^2(\mathbb{R})$  and we have  $g'(a; a) = 0$  for  $a \in \{0, 1\}$ ,  $g''(0; 0) > 0$  and  $g''(1; 1) < 0$ . Moreover, there exist  $a_0$  and  $a_1$  in  $(0, 1)$  such that for each  $a \in (0, a_0)$  and  $a \in (a_1, 1)$  there exists a unique  $v = v(a)$  for which  $g''(v; a) = 0$ .

Both (Hg1) and (Hg2) are satisfied for the standard cubic nonlinearity (1.2), on account of the identities

$$\partial_a g(v; a) = -v(1-v) < 0, \quad g'(a; a) = -a^2 + a, \quad g''(a; a) = -2a + 1$$

and the fact that the equality  $g''(v; a) = 0$  holds if and only if  $v = (a+1)/3$ .

We are specially interested in so-called traveling wave solutions to (2.1), which can be written in the form

$$u_i(t) = \Phi(i - ct), \quad (2.3)$$

for some speed  $c \in \mathbb{R}$  and profile  $\Phi : \mathbb{R} \rightarrow \mathbb{R}$ . Substituting (2.3) into (2.1) results in the MFDE

$$-c\Phi'(\xi) = d(k\Phi(\xi+1) - (k+1)\Phi(\xi) + \Phi(\xi-1)) + g(\Phi(\xi); a). \quad (2.4)$$

Throughout most of the paper we restrict ourselves to heteroclinic connections that connect the two stable equilibria of the nonlinearity  $g$ . Therefore, we also add the boundary conditions

$$\lim_{\xi \rightarrow -\infty} \Phi(\xi) = 0, \quad \lim_{\xi \rightarrow +\infty} \Phi(\xi) = 1. \quad (2.5)$$

Equation (2.4) is a special case of the general problem considered in [19]. We therefore start by summarizing the key results from [19] that we use in our work. To simplify our notation, we write

$$\mathcal{H} = (0, 1) \times (0, \infty)$$

for the set of parameters  $(a, d)$  that we consider.

**Proposition 2.1.** [19, Thm. 2.1] *Suppose that (Hg) holds and pick  $(a, d) \in \mathcal{H}$  together with  $k > 0$ . Then there exist a speed  $c = c(a, d, k)$  and a non-decreasing profile  $\Phi : \mathbb{R} \rightarrow \mathbb{R}$  that solve (2.4) with the boundary conditions (2.5). Moreover,  $c(a, d, k)$  is uniquely determined and depends  $C^1$ -smoothly on all parameters when  $c(a, d, k) \neq 0$ . In this case the profile  $\Phi$  is  $C^1$ -smooth with  $\Phi' > 0$  and unique up to translations.*

In the traditional setting where  $k = 1$  and  $g$  is given by the cubic nonlinearity (1.2), one can exploit the identity  $g(1 - v; a) = -g(v; 1 - a)$  to obtain the symmetry relation

$$c(a, d, 1) = -c(1 - a, d, 1). \quad (2.6)$$

This allows the analysis in [15] to only consider one of the cases  $c < 0$  or  $c > 0$  and subsequently transfer the results to the other case.

The result below provides a useful generalization of this symmetry relation, which will help to interpret and formulate some of our results. As a preparation, we introduce the transformed parameters

$$\tilde{k} = \frac{1}{k}, \quad \tilde{a} = 1 - a, \quad \tilde{d} = dk, \quad (2.7)$$

together with the nonlinearity

$$\tilde{g}(v; \tilde{a}) = -g(1 - v; a). \quad (2.8)$$

Since the function  $\tilde{g}$  also satisfies (Hg), Proposition 2.1 yields the existence of a transformed speed function  $\tilde{c}$  associated to the solutions of (2.4)-(2.5) with  $(\tilde{k}, \tilde{a}, \tilde{d}, \tilde{g})$  instead of  $(k, a, d, g)$ .

**Lemma 2.2.** *Suppose that (Hg) holds and pick  $(a, d) \in \mathcal{H}$  together with  $k > 0$ . Then we have*

$$\tilde{c}(\tilde{a}, \tilde{d}, \tilde{k}) = -c(a, d, k). \quad (2.9)$$

*Proof.* Let  $(c, \Phi)$  be a solution of the MFDE (2.4)-(2.5) and write  $\tilde{\Phi}(\xi) = 1 - \Phi(-\xi)$  together with  $\tilde{c} = -c$ . A straightforward computation shows that the pair  $(\tilde{c}, \tilde{\Phi})$  also satisfies (2.4)-(2.5), but now with the transformed parameters (2.7) and nonlinearity (2.8).  $\square$

## 2.1 Pinned waves

In our following result we show that for any bistable nonlinearity there exists a nonempty region in the  $(a, d)$  plane where waves are pinned, i.e.,  $c = 0$ , see Fig. 4. We achieve this by showing that there exist two regions with nonempty intersection, one with  $c \leq 0$  and the other with  $c \geq 0$ . To this end, we define two curves  $d^- : (0, 1) \rightarrow (0, \infty)$  and  $d^+ : (0, 1) \times (0, \infty) \rightarrow (0, \infty)$  by writing

$$d^-(a) := \max_{y \in (a, 1)} \frac{g(y; a)}{y}, \quad d^+(a, k) := \max_{y \in (1-a, 1)} \frac{-g(1-y; a)}{ky}. \quad (2.10)$$

We note that the  $k$ -dependence of  $d^+$  is directly related to the transformation (2.7). Finally, we define the analytical pinning region by

$$\mathcal{D}^0(k) := \{(a, d) \in \mathcal{H} : 0 < d < \min\{d^-(a), d^+(a, k)\}\}. \quad (2.11)$$

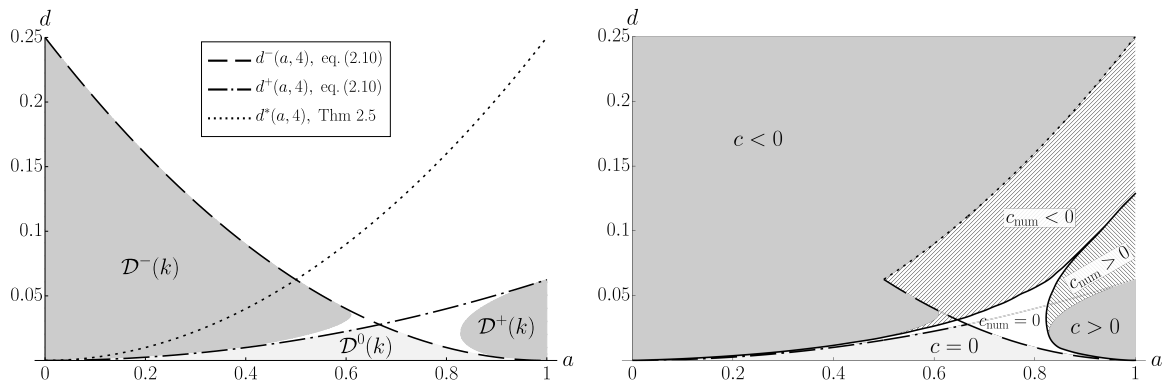


Figure 4: Our analytical and numerical results for the cubic (1.2) and  $k = 4$ . The left panel shows the analytical regions  $\mathcal{D}^0(k)$ ,  $\mathcal{D}^-(k)$  and  $\mathcal{D}^+(k)$  for which we prove  $c = 0$ ,  $c < 0$  and  $c > 0$ , respectively (see Propositions 2.3, 2.9 and Corollary 2.10). Moreover, for  $d > d^*(a, 4)$  the negative speed  $c < 0$  is implied by Theorem 2.5. In the right panel these analytical regions (gray) are accompanied by the numerical regions (hatched for  $c \neq 0$  and white for  $c = 0$ ). Compare with Fig. 2.

**Proposition 2.3.** *Assume that (Hg) holds and pick  $a \in (0, 1)$  together with  $k > 0$ . Then the following claims hold true.*

(i) *For any  $d \in (0, d^+(a, k))$  we have  $c(a, d, k) \geq 0$ .*

(ii) *For any  $d \in (0, d^-(a))$  we have  $c(a, d, k) \leq 0$ .*

*In particular, for any  $(a, d) \in \mathcal{D}^0(k)$  we have  $c(a, d, k) = 0$ .*

As a follow-up result, we provide more detailed insight into the pinning region. We show that for all sufficiently small  $d > 0$  one can construct infinitely many bounded solutions to (2.4) with  $c = 0$ . This system is said to admit ‘spatial chaos’ due to the fact that these solutions can be constructed from arbitrary sequences in  $\{0, 1\}$ .

**Proposition 2.4.** *Assume that (Hg) holds and pick  $a \in (0, 1)$  together with  $k > 0$ . Then there exists  $d_0 = d_0(a, k) > 0$  such that for every  $0 < d \leq d_0$  and every sequence  $(s_i)_{i \in \mathbb{Z}} \subset \{0, 1\}$ , there is at least one solution of (2.4) that has  $c = 0$  together with*

$$\begin{aligned} \Phi(i) &\in [0, a), & \text{if } s_i = 0, \\ \Phi(i) &\in (a, 1], & \text{if } s_i = 1. \end{aligned}$$

## 2.2 Propagating waves

The two main results below establish criteria that guarantee the propagation of waves, i.e.,  $c \neq 0$ . The first one provides a quantitative lower bound  $d^*$  above which the wave speed is strictly negative. This lower bound is defined for all  $k > 1$  and  $a \in (0, 1)$ , in clear contrast to the symmetry (2.6) that occurs for the cubic nonlinearity with  $k = 1$ . We note that general conditions that guarantee  $c > 0$  for  $k = 1$  and  $a \sim 1$  can be found in [19, Thm. 2.6].

**Theorem 2.5.** *Assume that (Hg) holds. Pick  $a \in (0, 1)$  together with  $k > 1$  and define the quantity*

$$d^*(a, k) = (1 - k^{-1/2})^{-2} d^+(a, k) \quad (2.12)$$

*Then for any  $d > d^*(a, k)$  we have  $c(a, d, k) < 0$ .*

Our second main result provides an alternative set of criteria that guarantee both strictly positive and negative wave speeds. Our numerical results for the cubic nonlinearity (1.2) show that the



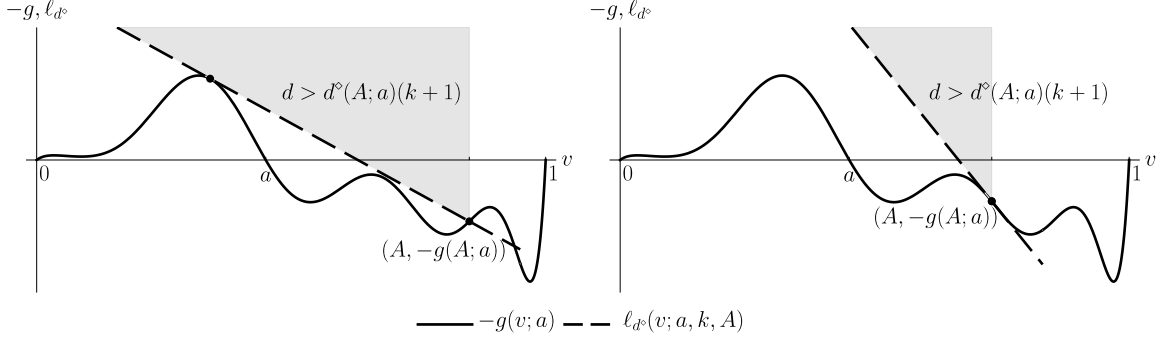


Figure 5: In the left panel, the value of  $d^\circ = d^\circ(A; a)$  is determined by the tangential intersection of the line and the graph of  $-g$  at a point  $v \leq A$ . In the right panel we have  $-d^\circ(A; a)(k+1) = g'(A; a)$ .

boundary of the associated parameter sets track the edge of the pinning region rather well for a wide range of parameters  $a$ ; see Fig. 4.

The characterization of these sets depend on a geometric construction involving the graph of the nonlinearity  $g$ . To describe this construction, we pick parameters  $k > 0$ ,  $a \in (0, 1)$ ,  $A \in (0, 1)$ ,  $d > 0$  and define a linear map  $\ell_d(\cdot; a, k, A) : (0, 1) \rightarrow \mathbb{R}$  that acts as

$$\ell_d(v; a, k, A) := d(k+1)(A-v) - g(A; a). \quad (2.13)$$

This linear map intersects the graph of  $-g$  at  $v = A$  and slopes downward with a steepness that is proportional to  $d$ . The smoothness of  $g$  now allows us to define

$$d^\circ(A; a) = \inf\{d > 0 : \ell_d(v; a, k, A) \geq -g(v; a), \text{ for all } v \in [0, A]\}, \quad (2.14)$$

representing the minimal value of  $d$  that is required to ensure that  $\ell_d$  stays above the graph of  $-g$  on  $[0, A]$ ; see Fig. 5.

We now define the set  $\mathcal{D}^- \subset \mathcal{H}$  by writing

$$\mathcal{D}^-(k) = \mathcal{D}_g^-(k) := \left\{ (a, d) \in \mathcal{H} : d^\circ(A; a) < d < \frac{g(A; a)}{A} \text{ for some } A \in (a, 1) \right\}, \quad (2.15)$$

using the subscript only when required for explicitness. We will show that  $c < 0$  on  $\mathcal{D}^-$ , which is a priori bounded from above by the function  $d^-(a)$  defined in (2.10). To tackle the opposite case  $c > 0$ , we exploit the symmetry (2.9) and define the set

$$\mathcal{D}^+(k) = \left\{ (a, d) \in \mathcal{H} : (\tilde{a}, \tilde{d}) \in \mathcal{D}_g^-\left(\tilde{k}\right) \right\}. \quad (2.16)$$

Upon introducing the notation (symmetrical to (2.14))

$$\tilde{d}^\circ(A; a) = \inf \left\{ \tilde{d} > 0 : \tilde{d} \left(1 + \frac{1}{k}\right) (A-v) + g(1-A; a) \geq g(1-A; a), \text{ for all } v \in [0, A] \right\}, \quad (2.17)$$

the definition (2.16) can be recast in the form

$$\mathcal{D}^+(k) = \left\{ (a, d) \in \mathcal{H} : \frac{\tilde{d}^\circ(A; a)}{k} < d < -\frac{g(1-A; a)}{kA} \text{ for some } A \in (1-a, 1) \right\},$$

which only involves the original nonlinearity. Notice again that this set is a priori bounded from above by the function  $d^+(a, k)$  defined in (2.10).

**Theorem 2.6.** *Assume that (Hg) is satisfied and pick  $k > 0$ . Then the following claims hold true.*

- (i) *We have  $\mathcal{D}^-(k) \neq \emptyset$  and  $\mathcal{D}^+(k) \neq \emptyset$ .*

(ii) For all  $(a, d) \in \mathcal{D}^-(k)$  we have  $c(a, d, k) < 0$ . Equivalently, for all  $(a, d) \in \mathcal{D}^+(k)$  we have  $c(a, d, k) > 0$ .

(iii) Assume that (Hg1) holds and pick any  $(a, d) \in \overline{\mathcal{D}^-} \cap \mathcal{H}$ . Then we have  $c(a', d) < 0$  for all  $0 < a' < a$ . Similarly, pick any  $(a, d) \in \overline{\mathcal{D}^+} \cap \mathcal{H}$ . Then we have  $c(a', d) > 0$  for all  $a < a' < 1$ .

(iv) Assume that (Hg2) holds. Then there exists  $\delta_a \in (0, 1)$  such that

$$\left( a, \frac{g'(a; a)}{k+1} \right) \in \begin{cases} \mathcal{D}^-(k), & \text{for } a \in (0, \delta_a), \\ \mathcal{D}^+(k), & \text{for } a \in (1 - \delta_a, 1). \end{cases} \quad (2.18)$$

Note that the condition (Hg1) implies that we can fully characterize  $\mathcal{D}^-$  and  $\mathcal{D}^+$  by finding their right and left boundaries, respectively. In addition, the assumption (Hg2) guarantees that the set  $\mathcal{D}^-$  extends to the corner  $(a, d) = (0, 0)$ , while  $\mathcal{D}^+$  extends to  $(a, d) = (1, 0)$ .

### 2.3 Cubic nonlinearity

In this subsection we apply our techniques to the standard cubic nonlinearity (1.2). In particular, we obtain explicit expressions for the curves and regions that appear in our main results. First, we describe the functions  $d^\pm$  and  $d_0$  that characterize the pinning region and the chaotic behaviour therein. As an immediate consequence we also get an explicit expression for the curve  $d^*$ , above which the wave speed is guaranteed to be negative.

**Lemma 2.7.** *Let  $g$  be the standard cubic nonlinearity (1.2). Then the explicit expressions for the functions  $d^-$  and  $d^+$  defined by (2.10) are given by*

$$d^-(a) = \frac{(1-a)^2}{4}, \quad d^+(a, k) = \frac{a^2}{4k}.$$

*Proof.* This claim follows from a straightforward analysis of quadratic expressions.  $\square$

**Proposition 2.8.** *Let  $g$  be the standard cubic nonlinearity (1.2) and pick parameters  $k > 0$  and  $a \in (0, 1)$ . Then the following claims hold true.*

(i) Pick any  $d > 0$  that satisfies

$$d < \min \left\{ \frac{a^2}{4k}, \frac{(1-a)^2}{4} \right\} = \begin{cases} \frac{a^2}{4k}, & a \leq \frac{1}{1/\sqrt{k}+1}, \\ \frac{(1-a)^2}{4}, & a \geq \frac{1}{1/\sqrt{k}+1}. \end{cases}$$

Then we have  $c(a, d, k) = 0$ .

(ii) The function  $d_0$  from Proposition 2.4 is given by

$$d_0(a, k) := \frac{1}{k+1} \min \{ kd^+(a, k), d^-(a) \}. \quad (2.19)$$

In particular, for any  $k > 0$ ,  $a \in (0, 1)$  and  $0 < d < d_0(a, k)$  there exist infinitely many bounded solutions to (2.4) with  $c = 0$ .

(iii) Assume that  $k > 1$  and pick any  $d$  that satisfies

$$d > \frac{a^2}{4(\sqrt{k}-1)^2}.$$

Then we have  $c(a, d, k) < 0$ .

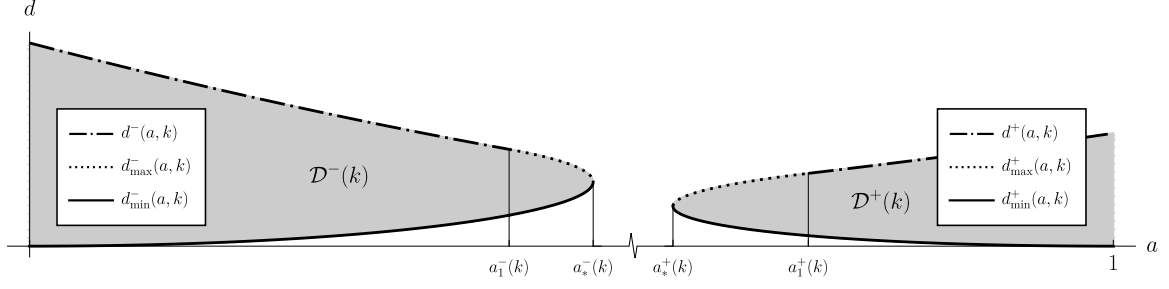


Figure 6: Curves and quantities defining regions  $\mathcal{D}^-(k)$  and  $\mathcal{D}^+(k)$ , see Propositions 2.8, 2.9 and Corollary 2.10. For a wider context, see Fig. 4.

*Proof.* The proof of items (i) and (iii) follows directly from Proposition 2.3 and Theorem 2.5 applied to Lemma 2.7. For the proof of (ii), see §8.  $\square$

We now set out to find explicit expressions for  $\mathcal{D}^-$  and  $\mathcal{D}^+$ . Item (iii) of Theorem 2.6 shows that it suffices to find the outer boundaries of these sets. To this end, we first define the quantities

$$a_*^-(k) := 1 - \frac{2}{\sqrt{4k+1}+1}, \quad a_1^-(k) := \max \left\{ 1 - \frac{2}{2\sqrt{k+1}}, 0 \right\}, \quad (2.20)$$

for  $k > 0$ , together with the curves

$$d_{\min}^-(a, k) := \frac{2a^2k - a + 2k - 2(a+1)\sqrt{k}\sqrt{ka^2 - a(2k+1) + k}}{(4k+1)^2},$$

$$d_{\max}^-(a, k) := \begin{cases} \frac{(1-a)^2}{4}, & \text{if } a \in [0, a_1^-(k)], \\ \frac{2a^2k - a + 2k + 2(a+1)\sqrt{k}\sqrt{ka^2 - a(2k+1) + k}}{(4k+1)^2}, & \text{if } a \in [a_1^-(k), a_*^-(k)], \end{cases}$$

for  $k > 0$  and  $0 \leq a \leq a_*^-(k)$ . Together, these curves define the boundary of  $\mathcal{D}^-$ , see Fig. 6.

**Proposition 2.9.** *[Cubic nonlinearity, negative speed] Pick  $k > 0$  and let  $g$  be the standard cubic nonlinearity (1.2). Then the following claims hold.*

(i) We have  $d_{\min}^-, d_{\max}^- \in C([0, a_*^-(k)] \times (0, \infty); \mathbb{R})$  and

$$0 \leq d_{\min}^-(a, k) \leq d_{\max}^-(a, k) \leq d^-(a), \quad \text{for all } a \in [0, a_*^-(k)].$$

(ii) The equality  $d_{\max}^-(a_*^-(k)) = d_{\min}^-(a_*^-(k))$  holds.

(iii) The set  $\mathcal{D}^-(k)$  is bounded precisely by the graphs of  $d_{\min}^-$  and  $d_{\max}^-$ , namely

$$\mathcal{D}^-(k) = \{(a, d) \in \mathcal{H} : a < a_*^-(k), \quad d_{\min}^-(a, k) < d < d_{\max}^-(a, k)\}. \quad (2.21)$$

To formulate the equivalent result for the set  $\mathcal{D}^+$ , we again define two values

$$a_*^+(k) = \frac{\sqrt{4k+k^2} - k}{2}, \quad a_1^+(k) = \min \left\{ \frac{2\sqrt{k}}{2 + \sqrt{k}}, 1 \right\} \quad (2.22)$$

for  $k > 0$ , together with two curves

$$d_{\min}^+(a, k) := \frac{2a^2 + a(k-4) + 4 - k - \sqrt{a^2 + ka - k}}{(4+k)^2},$$

$$d_{\max}^+(a, k) := \begin{cases} \frac{a^2}{4k}, & \text{if } a \in (a_1^+(k), 1), \\ \frac{2a^2 + a(k-4) + 4 - k + \sqrt{a^2 + ka - k}}{(4+k)^2}, & \text{if } a \in [a_*^+(k), a_1^+(k)], \end{cases}$$

for  $k > 0$  and  $a_1^+(k) \leq a \leq 1$ . See Fig. 6 for illustration.

**Corollary 2.10.** [Cubic nonlinearity, positive speed] Pick  $k > 0$  and let  $g$  be the standard cubic nonlinearity (1.2). Then the following claims hold.

(i) We have  $d_{\min}^+, d_{\max}^+ \in C([a_*^+(k), 1] \times (0, \infty); \mathbb{R})$  and

$$0 \leq d_{\min}^+(a, k) \leq d_{\max}^+(a, k) \leq d^+(a, k), \quad \text{for all } a \in [0, a_*^+(k)].$$

(ii) The equality  $d_{\max}^+(a_*^+(k)) = d_{\min}^+(a_*^+(k))$  holds.

(iii) The set  $\mathcal{D}^+$  is bounded precisely by the graphs of  $d_{\min}^+$  and  $d_{\max}^+$ , namely

$$\mathcal{D}^+(k) = \{(a, d) \in \mathcal{H} : a > a_*^+(k), d_{\min}^+(a, k) < d < d_{\max}^+(a, k)\}. \quad (2.23)$$

*Proof.* This result follows directly from Proposition 2.9 and Lemma 2.2 by noting that

$$a_*^+(k) = 1 - a_*^-\left(\frac{1}{k}\right), \quad a_1^+(k) = 1 - a_1^-\left(\frac{1}{k}\right),$$

together with

$$d_{\min}^+(a, k) = \frac{d_{\min}^-(1-a, 1/k)}{k}, \quad d_{\max}^+(a, k) = \frac{d_{\max}^-(1-a, 1/k)}{k}.$$

□

### 3 Comparison principles

The main tool that we use in this paper to analyze the LDE (2.1) is the well-known comparison principle, which is formulated in the first result below. We will exploit this principle in a standard fashion to show that solutions with monotonic initial conditions remain monotonic. In addition, we show how the sign of the wave speed  $c(a, d, k)$  defined in Proposition 2.1 can be controlled by constructing appropriate lower and upper solutions.

**Lemma 3.1.** Let  $u, v \in C^1([0, \infty), \ell^\infty(\mathbb{Z}))$  be such that

$$\begin{aligned} \dot{u}_i(t) &\geq d[\Delta_k u(t)]_i + g(u_i(t); a), \\ \dot{v}_i(t) &\leq d[\Delta_k v(t)]_i + g(v_i(t); a) \end{aligned} \quad (3.1)$$

and  $u_i(0) \geq v_i(0)$  for all  $i \in \mathbb{Z}$ . Then  $u_i(t) \geq v_i(t)$  for  $t > 0$  and all  $i \in \mathbb{Z}$ .

*Proof.* The statement is the reformulation of [6, Lemma 1] with  $j = \infty$  and

$$\mathcal{N}_i u(t) = \dot{u}_i(t) - d[\Delta_k u(t)]_i - g(u_i(t); a).$$

□

**Lemma 3.2.** *Assume that (Hg) holds and pick a non-decreasing sequence  $u^0 \in \ell^\infty(\mathbb{Z})$ . Then the solution  $u(t)$  to the LDE (2.1) with  $u(0) = u^0$  is also a non-decreasing sequence for all  $t > 0$ .*

*Proof.* Define the function  $v(t)$  with  $v_i(t) = u_{i+1}(t)$ . Then this function also satisfies the LDE (2.1) and we have  $u_i^0 \leq v_i^0$  for each  $i \in \mathbb{Z}$ . By Lemma 3.1 this implies  $u_i(t) \leq v_i(t)$  for all  $i \in \mathbb{Z}$  and  $t > 0$ .  $\square$

In order to translate the inequalities (3.1) to the context of traveling waves, we introduce the operators  $\mathcal{I}_{a,d,k} : \mathbb{R} \times C^1(\mathbb{R}) \rightarrow C(\mathbb{R})$  that act as

$$\mathcal{I}_{a,d,k}[c, \Phi](\xi) := -c\Phi'(\xi) - d(\Phi(\xi - 1) - (k + 1)\Phi(\xi) + k\Phi(\xi + 1)) - g(\Phi(\xi); a). \quad (3.2)$$

This can be interpreted as the residual of the traveling-wave equation (2.4), i.e.,  $\mathcal{I}_{a,d,k}[c, \Phi] = 0$  if and only if the pair  $(c, \Phi)$  solves (2.4).

**Corollary 3.3.** *Pick  $k > 0$ , a pair  $(a, d) \in \mathcal{H}$  and a function  $g$  that satisfies (Hg). Let the pair  $(c, \Phi)$  be a solution of (2.4)-(2.5). Assume that there exist a constant  $\bar{c} \in \mathbb{R}$  and a bounded function  $\Psi \in C^1(\mathbb{R})$  that satisfy the properties*

- (i)  $\sup_{\xi \in \mathbb{R}} \Psi(\xi) > 0$  (resp.  $\inf_{\xi \in \mathbb{R}} \Psi(\xi) < 1$ ),
- (ii)  $\Psi(\xi) \leq \Phi(\xi)$  (resp.  $\Psi(\xi) \geq \Phi(\xi)$ ) for all  $\xi \in \mathbb{R}$ ,
- (iii)  $\mathcal{I}_{a,d,k}[\bar{c}, \Psi](\xi) \leq 0$  (resp.  $\mathcal{I}_{a,d,k}[\bar{c}, \Psi](\xi) \geq 0$ ) for all  $\xi \in \mathbb{R}$ .

Then we have  $c \leq \bar{c}$  (resp.  $c \geq \bar{c}$ ).

*Proof.* Without loss of generality, we consider the case  $\Psi \leq \Phi$ . Let us define two time-dependent sequences,  $v_i(t) := \Psi(i - \bar{c}t)$  and  $u_i(t) := \Phi(i - ct)$ , for  $i \in \mathbb{Z}$ . By construction, the assumptions of Lemma 3.1 are satisfied and we therefore have

$$\Psi(i - \bar{c}t) \leq \Phi(i - ct) \quad (3.3)$$

for all  $i \in \mathbb{Z}$  and  $t > 0$ .

To show that  $c \leq \bar{c}$ , we assume to the contrary that  $c > \bar{c}$ . Let  $\xi_0 \in \mathbb{R}$  be such that  $\Psi(\xi_0) = M > 0$ . Due to the shift-invariance of the MFDE (3.3), we can shift both  $\Psi$  and  $\Phi$  to have  $\xi_0 = 0$ . In addition, due to the first limit in (2.5) we can find an integer  $i_1 < 0$  so that  $\Phi(\xi) < M/2$  for all  $\xi \leq i_1$ . We now write

$$i_1 = -(c - \bar{c})t_1 \quad (3.4)$$

and pick  $t_2 \geq t_1 > 0$  in such a way that  $\bar{c}t_2 = i_2 \in \mathbb{Z}$ . We now have  $v_{i_2}(t_2) = \Psi(i_2 - \bar{c}t_2) = \Psi(0) = M$ . On the other hand, since

$$i_2 - ct_2 = (\bar{c} - c)t_2 \leq (\bar{c} - c)t_1 = i_1 \quad (3.5)$$

we have  $u_{i_2}(t_2) = \Phi(i_2 - ct_2) < M/2$ , which clearly contradicts (3.3).  $\square$

## 4 Pinned monotonic waves

In this section we follow the approach from [15] to establish Proposition 2.3. The series of Lemmas 4.1, 4.2 and 4.3 yield the existence of two invariant intervals  $(x_1, 1]$  and  $[0, y_2)$  for the LDE (2.1). More precisely, choosing  $(a, d) \in \mathcal{H}$  with  $d < d^-(a)$ , we have  $u_i(t) \in (x_1, 1]$  provided that  $u_i^0 \in (x_1, 1]$ . This feature blocks propagation to the right since traveling waves are known to be strictly monotonic [19]. On the other hand, the interval  $[0, y_2)$  is invariant for the LDE (2.1) when  $d < d^+(a, k)$ , which blocks propagation to the left.

**Lemma 4.1.** *Consider the setting of Proposition 2.3. Pick any  $a \in (0, 1)$  and  $d < d^-(a)$ . Then there exist two points  $x_1, x_2$ , with  $a < x_1 < x_2 < 1$  such that*

$$dy - g(y; a) < 0, \quad y \in (x_1, x_2). \quad (4.1)$$

*Proof.* Let us take  $d < d^-(a)$ . By definition of  $d^-$ , there exists  $x_0 \in (a, 1)$  such that

$$d < \frac{g(x_0; a)}{x_0}.$$

The strict inequality ensures that there exists an interval  $(x_1, x_2)$  around  $x_0$  such that (4.1) holds.  $\square$

**Lemma 4.2.** *Consider the setting of Proposition 2.3. Pick any  $a \in (0, 1)$  and  $d < d^+(a, k)$ . Then there exist two points  $y_1, y_2$  with  $1 - a < y_1 < y_2 < 1$  such that*

$$dky + g(1 - y; a) < 0, \quad y \in (y_1, y_2).$$

*Proof.* The proof is analogous to that of Lemma 4.1.  $\square$

**Lemma 4.3.** *Assume that (Hg) holds and pick a pair  $(a, d) \in \mathcal{H}$  together with a non-decreasing sequence  $u^0 \in \ell^\infty(\mathbb{Z})$  that has  $0 \leq u_i^0 \leq 1$  for all  $i \in \mathbb{Z}$ . Let  $u(t)$  be the solution to the LDE (2.1) with  $u(0) = u^0$ . Then the following claims hold.*

(i) *If  $d < d^+(a, k)$  and  $u_i^0 \in [0, y_2)$  for some  $i \in \mathbb{Z}$ , then  $u_i(t) \in [0, y_2)$  for all  $t > 0$ .*

(ii) *If  $d < d^-(a)$  and  $u_i^0 \in (x_1, 1]$  for some  $i \in \mathbb{Z}$ , then  $u_i(t) \in (x_1, 1]$  for all  $t > 0$ .*

*Proof.* By the comparison principle we have  $u_i(t) \in [0, 1]$  for all  $t > 0$ . By Lemma 3.2 we also know that  $u_i(t)$  is a monotonic sequence for all  $t > 0$ . Assume that  $u_i^0 \in [0, y_2)$  and that there exists  $t > 0$  such that  $u_i(t) \geq y_2$ . A continuity argument ensures that there exists  $t_0 > 0$  such that  $u_i(t_0) \in (y_1, y_2)$  and  $\dot{u}_i(t_0) \geq 0$ . However, by Lemma 4.2, we have

$$\begin{aligned} \dot{u}_i(t_0) &= d(u_{i-1}(t_0) - u_i(t_0) + k(u_{i+1}(t_0) - u_i(t_0))) + g(u_i(t_0); a) \\ &\leq d(k(1 - u_i(t_0))) + g(u_i(t_0); a) < 0, \end{aligned}$$

which contradicts our assumption  $\dot{u}_i(t_0) \geq 0$ . This proves item (i). Item (ii) follows similarly.  $\square$

*Proof of Proposition 2.3.* In view of Proposition 2.1, we can find a solution  $(\Phi, c)$  to (2.4)-(2.5). Setting

$$u_i^0 := \Phi(i),$$

we see that  $u^0$  is a non-decreasing sequence connecting 0 and 1. Let  $I_1 \in \mathbb{Z}$  be such that

$$\Phi(i) < y_2, \quad i \leq I_1.$$

Assume now that  $0 < d < d^+(a, k)$ . By item (i) of Lemma 4.3 the associated wave solution  $u_i(t) = \Phi(i - ct)$  has  $u_i(t) < y_2$  for all  $t > 0$  and  $i \leq I_1$ , which implies  $c \geq 0$ . Item (ii) follows analogously.  $\square$

## 5 Small $d$ regime

The main goal of this section is to establish Theorem 2.6 by constructing appropriate sub-solutions. In light of the a priori upper bounds for the regions  $\mathcal{D}^-$  and  $\mathcal{D}^+$ , we consider this the ‘small  $d$ ’-regime. The geometric interpretation that we develop here will allow us to find explicit characterizations for these sets in §7 in the special case that  $g$  is the standard cubic nonlinearity (1.2).

Following the approach developed by Keener [15], we fix  $a \in (0, 1)$  and  $A \in (a, 1)$  and set out to construct a smooth but steep sub-solution  $\Psi$  that connects zero to  $A$ , see Fig. 3. We first show that the corresponding sub-solution residual can be controlled by the expression

$$\mathcal{J}^-(a, d, A, k) := \max_{v \in [0, A]} (d(k+1)v - dkA - g(v; a)), \quad (5.1)$$

which forces  $c(a, d, k) < 0$  whenever it is negative.

**Lemma 5.1.** *Consider the setting of Theorem 2.6. Pick  $(a, d) \in \mathcal{H}$  and suppose that there exists  $A \in (a, 1)$  with the property  $\mathcal{J}^-(a, d, A, k) < 0$ . Then we have  $c(a, d, k) < 0$ .*

*Proof.* The strict inequality  $A < 1$  allows us to choose  $\xi_0$  and  $\xi_1$  so that

$$\Phi(\xi_0) > A \quad \text{and} \quad 0 < \xi_1 - \xi_0 < 1.$$

We use  $\xi_0$  and  $\xi_1$  to define a smooth function  $\Psi : \mathbb{R} \rightarrow \mathbb{R}$  that satisfies

$$\Psi(\xi) = \begin{cases} 0, & \xi \leq \xi_0, \\ A, & \xi \geq \xi_1, \end{cases} \quad (5.2)$$

and is strictly increasing for  $\xi_0 < \xi < \xi_1$ . We will show that there exists  $\bar{c} < 0$  such that

$$\mathcal{I}_{a,d,k}(\bar{c}, \Psi) \leq 0,$$

which yields  $c(a, d, k) < 0$  using Corollary 3.3.

To this end, we define

$$\epsilon := \min_{v \in [0, A]} g(v; a) + d(kA - (k+1)v) > 0, \quad (5.3)$$

which allows us to choose  $\bar{c} < 0$  in such a way that

$$|\bar{c}\Psi'(\xi)| \leq \epsilon.$$

For  $\xi < \xi_0$  we have  $\Psi'(\xi) = 0$  and

$$\mathcal{I}_{a,d,k}(\bar{c}, \Psi) \leq -dk\Psi(\xi+1) \leq 0.$$

If  $\xi > \xi_1$  we again have  $\Psi'(\xi) = 0$  and

$$\mathcal{I}_{a,d,k}(\bar{c}, \Psi) \leq dA - g(A; a) < 0.$$

For  $\xi \in [\xi_0, \xi_1]$  we have  $\Psi(\xi) \in [0, A]$ ,  $\Psi(\xi-1) = 0$  and  $\Psi(\xi+1) = A$ , which gives

$$\mathcal{I}_{a,d,k}(\bar{c}, \Psi) \leq \epsilon - d(kA - (k+1)\Psi(\xi)) - g(\Psi(\xi); a) \leq 0,$$

as desired.  $\square$

A key ingredient towards establishing Theorem 2.6 is to find an explicit relation between the set  $\mathcal{D}^-$  and the expression  $\mathcal{J}^-$ . This is achieved in the following result, using a geometric construction that is illustrated in Fig. 7.

**Proposition 5.2.** *Consider the setting of Theorem 2.6. Then the following two statements are equivalent.*

- (i) *We have  $(a, d) \in \mathcal{D}^-(k)$ .*
- (ii) *There exists  $A \in (a, 1)$  for which  $\mathcal{J}^-(a, d, A, k) < 0$ .*

*Proof.* Assuming (i), there exists  $A \in (a, 1)$  so that for all  $v \in [0, A]$  we have  $d(k+1)(A-v) - g(A; a) \geq -g(v; a)$ . Since also  $dA < g(A; a)$ , this implies that

$$\begin{aligned} \mathcal{J}^-(a, d, A, k) &= d(k+1)(v-A) + dA - g(v; a) \\ &< d(k+1)(v-A) - g(A; a) - g(v; a) \leq 0. \end{aligned}$$

To establish the opposite inclusion, we assume (ii) and write  $\underline{A} = \frac{k}{k+1}A$ . The line through  $(\underline{A}, 0)$  with slope  $-d(k+1)$  intersects the graph of  $-g$  at some point  $v = A_2 > A$ , see Fig. 7. We automatically have  $d > d^\circ(A_2; a)$  by definition of  $d^\circ(A_2; a)$  in (2.14), so it suffices to show that  $d < g(A_2; a)/A_2$ .

To this end, we write  $\underline{A}_2 = \frac{k}{k+1}A_2$  and point out that the slope of the line connecting the points  $(\underline{A}_2, 0)$  and  $(A_2, -g(A_2; a))$  is given by  $\underline{d} = -\frac{g(A_2; a)}{A_2}(k+1)$ . Since we have  $\underline{A}_2 > \underline{A}$ , the inequality  $-d(k+1) > -\underline{d}$  must also hold, which immediately implies  $d < g(A_2; a)/A_2$ .  $\square$

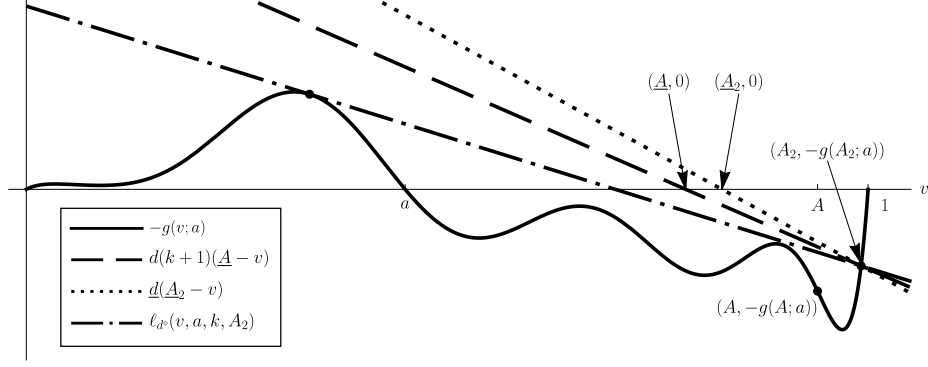


Figure 7: The geometric intuition behind the ideas and quantities from the proof for Proposition 5.2. Note that  $d^\circ(k+1) < d(k+1) < \underline{d}$ .

We now continue with two essential observations concerning the quantities  $d^\circ$  and  $\mathcal{J}^-$ . These will allow us to conclude that  $\mathcal{D}^-$  is non-empty and - when (Hg1) holds - free of holes.

**Lemma 5.3.** *Consider the setting of Theorem 2.6. There exist  $0 < A^* < 1$  and  $a_- > 0$  such that for all  $a \in (0, a_-)$  we have*

$$d^\circ(A^*; a) < \frac{g(A^*; a)}{A^*}. \quad (5.4)$$

*Proof.* We first note that it suffices to find  $0 < A^* < 1$  for which (5.4) holds at  $a = 0$ . Indeed,  $g(A; a)/A$  and  $d^\circ(A; a)$  are continuous with respect to both their arguments, the latter since it is the supremum of a difference quotient on a compact interval that depends continuously on these arguments.

To show this, we define

$$\epsilon = \frac{k}{8(k+1)}$$

and use the fact that  $g'(1; 0) < 0$  to pick  $A_* \in (1/2, 1)$  in such a way that the line connecting the points  $(A_*, -g(A_*; 0))$  and  $(\epsilon, 0)$  is above the graph of  $-g(\cdot; 0)$  on  $[0, A]$ . The slope of this line is given by  $d_\epsilon = -\frac{g(A_*; 0)}{A_* - \epsilon}$ , which using the fact that  $kA - (k+1)\epsilon > 0$  implies

$$d^\circ(A_*; 0) \leq \frac{d_\epsilon}{k+1} = \frac{g(A_*; 0)}{(k+1)(A_* - \epsilon)} < \frac{g(A_*; 0)}{A_*},$$

as desired.  $\square$

**Lemma 5.4.** *Consider the setting of Theorem 2.6 and assume furthermore that (Hg1) is satisfied. Pick  $(a, d) \in \overline{\mathcal{D}^-} \cap \mathcal{H}$  and  $\underline{a} \in (0, a)$ . Then we have  $(\underline{a}, d) \in \mathcal{D}^-$ .*

*Proof.* By Proposition 5.2 we have

$$\mathcal{D}^-(k) = \bigcup_{a \in (0, 1)} \bigcup_{A \in (a, 1)} \{(a, d) \in \mathcal{H} : \mathcal{J}^-(a, d, A, k) < 0\}.$$

Let us now pick  $(a, d) \in \overline{\mathcal{D}^-} \cap \mathcal{H}$ . The continuity of  $\mathcal{J}^-$  with respect to  $A$  implies that

$$\mathcal{J}^-(a, d, A, k) \leq 0$$

holds for some  $A \in (a, 1]$ . Note that  $A = a$  is excluded here since  $\mathcal{J}^- = da$  for  $A = a$ .

For  $\bar{a} < a$ , the assumption (Hg1) implies that

$$g(v; \bar{a}) + d(kA - (k+1)v) > g(v; a) + d(kA - (k+1)v) \geq 0, \quad v \in (0, A],$$

while for  $v = 0$  we have  $g(0; \bar{a}) + dkA = dkA > 0$ . Therefore,  $\mathcal{J}^-(\bar{a}, d, A, k) < 0$  holds.  $\square$



In the following lemma we explore how the extra condition (Hg2) leads to the explicit inclusion  $(a, g'(a; a)/(k+1)) \in \mathcal{D}^-(k)$  for  $a \approx 0$ . In particular, translated into the language of  $d^\circ$ , the first item implies that  $g'(a; a)/(k+1) > d^\circ(A; a)$  for any  $A \in (a, 1)$ . The second item then ensures that there exists  $A$  such that  $d^\circ(A; a) < g(A; a)/A$ .

**Lemma 5.5.** *Pick  $k > 0$  and assume that the nonlinearity  $g$  satisfies (Hg) and (Hg2). Then there exist a constant  $\delta_a \in (0, 1)$  such that for all  $a \in (0, \delta_a)$  we have*

$$(i) \quad g''(a; a) > 0,$$

$$(ii) \quad 0 < \frac{g'(a; a)}{k+1} < \max_{A \in [a + \frac{2a}{k}, 1]} \frac{g(A; a)}{A}.$$

*Proof.* Due to the assumption (Hg), the function

$$D_-(a) = \max_{A \in [a + \frac{2a}{k}, 1]} \frac{g(A; a)}{A}$$

is well defined, positive and decreasing for  $a \leq 1/(k+2)$ . In particular, we have  $D_-(0) > 0$ . The assumption (Hg2) ensures that  $0 = g'(0, 0) < D_-(0)(k+1)$ . Now the existence of  $\delta_a$  and the claim of item (ii) follow from the continuity properties of the nonlinearity  $g$  and the function  $D_-$ . The inequality  $g''(a; a) > 0$  for  $a \in (0, \delta_a)$  follows again from (Hg2) by reducing  $\delta_a$  if necessary.  $\square$

*Proof of Theorem 2.6.* Item (i) follows directly from Lemma 5.3. To show item (ii), we first employ Proposition 5.2 in combination with Lemma 5.1 to conclude that  $c < 0$  in  $\mathcal{D}^-$ . The result  $c > 0$  in  $\mathcal{D}^+$  now follows from Lemma 2.2.

Item (iii) for  $\mathcal{D}^-$  is a direct consequence of Lemma 5.4 and Proposition 5.2. To show the equivalent result for  $\mathcal{D}^+$ , we assume that  $(a, d) \in \mathcal{D}^+$  and take  $\bar{a} > a$ . In view of the definition (2.16) for  $\mathcal{D}^+$ , we have  $(1-a, dk) \in \mathcal{D}^-(\tilde{g}, 1/k)$  and consequently  $(1-\bar{a}, dk) \in \mathcal{D}^-(\tilde{g}, 1/k)$ . In particular, this implies  $(\bar{a}, d) \in \mathcal{D}^+$ .

To show item (iv), we take  $\delta_a$  from Lemma 5.5 and implicitly define the quantity  $A^* \geq a + 2a/k$  by writing

$$\frac{g(A^*; a)}{A^*} = \max_{A \in [a + \frac{2a}{k}, 1]} \frac{g(A; a)}{A}.$$

For  $d = d(a) := g'(a; a)/(k+1)$ , the function  $g_1(v; a)$  defined by

$$g_1(v; a) = -g(v; a) - d(kA^* - (k+1)v) \tag{5.5}$$

satisfies  $g_1(0; a) < 0$  and  $g_1(A^*; a) = -g(A^*; a) + dA^* < 0$  by Lemma 5.5. Moreover, its unique local maximum or inflection point is achieved at  $v = a$  since

$$g_1'(a; a) = -g'(a; a) + (k+1)d = 0 \quad \text{and} \quad g_1''(a; a) = -g''(a; a) < 0.$$

The value in the local minimum is  $g_1(a; a) = -d(kA^* - (k+1)a) \geq -ad/k > 0$ . Therefore, we have  $\mathcal{J}^-(a, d, A^*, g, k) < 0$ , which implies  $c(a, d, k) < 0$  by Lemma 5.1 and Proposition 5.2.

To show that  $(a, d(a)) \in \mathcal{D}^+(k)$  for  $a \approx 1$ , where  $d(a) = g'(a; a)/(k+1)$  it suffices to show that  $(\tilde{a}, \tilde{d}(\tilde{a})) \in \mathcal{D}_{\tilde{g}}^-(1/k)$ . We note now that the nonlinearity  $\tilde{g}$  also satisfies (Hg) and (Hg2). Therefore, by repeating the procedure above, we have

$$\tilde{d}(\tilde{a}) = \frac{\tilde{g}'(\tilde{a}; \tilde{a})}{\tilde{k}+1} \in \mathcal{D}_{\tilde{g}}^-(\tilde{k}).$$

Translating back to our original coordinates we obtain

$$d(a) = \frac{\tilde{d}(\tilde{a})}{k} = \frac{g'(a; a)}{k+1} \in \mathcal{D}_g^+(k).$$

$\square$

## 6 Large $d$ regime

In this section, we prove Theorem 2.5 and show that the profile (2.3) satisfies  $c < 0$  if  $d \gg 0$ . We achieve this by applying Corollary 3.3 to a second class of sub-solutions  $\Psi$ , which have milder growth than those from §5. Using the notation (2.2) for the discrete diffusion-advection operator we use

$$\Delta_k[\Phi](\xi) := \Phi(\xi - 1) - (k + 1)\Phi(\xi) + k\Phi(\xi + 1), \quad (6.1)$$

which allows us to rewrite (3.2) as

$$\mathcal{I}_{a,d,k}[c, \Phi] = -c\Phi' - d\Delta_k[\Phi] - g(\Phi, a).$$

Since the term  $\Delta_k[\Psi]$  appears with a negative sign in the residual expression  $\mathcal{I}_{a,d,k}$ , our goal is to construct a simple subsolution  $\Psi$  with a strictly positive sign of  $\Delta_k[\Psi]$ . By choosing  $d > 0$  large enough the contribution of  $d\Delta_k[\Psi]$  can then be used to overcome the impact of the nonlinearity  $g$ .

We approach the construction of the profile  $\Psi$  in a stepwise fashion. First of all, for  $l > 1$  and  $A > 0$  we define the function  $\kappa_{l,A} : \mathbb{R} \rightarrow \mathbb{R}$  by writing

$$\kappa_{l,A}(\xi) = A(1 - l^{-\xi}). \quad (6.2)$$

One can directly compute that  $\kappa_{l,A}$  is strictly increasing with

$$\Delta_k[\kappa_{l,A}] = Al^{-\xi}(k - l)\left(1 - \frac{1}{l}\right). \quad (6.3)$$

We therefore have  $\Delta_k[\kappa_{l,A}] > 0$  if and only if  $l \in (1, k)$ . However, both  $\kappa_{l,A}$  and its derivative  $\kappa'_{l,A}(\xi)$  are unbounded as  $\xi \rightarrow -\infty$ , which prevents us from controlling the sign of  $\mathcal{I}_{a,d,k}$ .

To circumvent this drawback we define a modified profile

$$\Psi_{l,A}(\xi) = \begin{cases} A\left(1 - l - \frac{\log(l)}{3}\right), & \xi \leq -1 - \frac{1}{l}, \\ Ap_l(\xi), & -1 - \frac{1}{l} < \xi \leq -1, \\ \kappa_{l,A}(\xi), & \xi > -1 \end{cases} \quad (6.4)$$

in which  $p_l(\xi)$  is the cubic polynomial given by

$$p_l(\xi) = \frac{1}{3} \log(l)(l\xi + (1 + l))^3 + 1 - l - \frac{\log(l)}{3}.$$

It can be verified by a direct computation that the profile  $\Psi_{l,A}$  is  $C^1$ -smooth. The profile  $\Psi$  has a bounded derivative

$$0 \leq \Psi'_{l,A}(\xi) \leq \Psi'_{l,A}(-1) = \kappa'_{l,A}(-1) = Al \log(l), \quad \xi \in \mathbb{R}. \quad (6.5)$$

On account of the cubic polynomial  $p_l$  it is rather cumbersome to provide a precise expression for  $\Delta_k[\Psi_{l,A}]$ . We rather point out several key qualitative features, which guarantee that this expression is non-negative and are used later in the proof of Lemma 6.2.

**Lemma 6.1.** *Pick  $k > 1$  together with  $l \in (1, k)$  and  $A \in (0, 1)$ . Then*

- (i)  $\Delta_k[\Psi_{l,A}](\xi) = 0$  for  $\xi \leq -2 - \frac{1}{l}$ ,
- (ii)  $\Delta_k[\Psi_{l,A}](\xi)$  is strictly increasing for  $\xi \in (-2 - \frac{1}{l}, -1 - \frac{1}{l}]$ ,
- (iii)  $\Delta_k[\Psi_{l,A}](\xi)$  is concave for  $\xi \in (-1 - \frac{1}{l}, -1)$ ,
- (iv)  $\Delta_k[\Psi_{l,A}](\xi) > \Delta_k[\kappa_{l,A}](\xi)$  for  $\xi \in [-1, 0)$ ,
- (v)  $\Delta_k[\Psi_{l,A}](\xi) = \Delta_k[\kappa_{l,A}](\xi)$  for  $\xi \geq 0$ .

*Proof.* The claims (i) and (v) follow directly from the definitions (6.1) and (6.4). To establish (ii), we pick  $\xi \in (-2 - \frac{1}{l}, -1 - \frac{1}{l}]$  and note that  $\Psi_{l,A}(\xi - 1) = \Psi_{l,A}(\xi) = A \left(1 - l - \frac{\log(l)}{3}\right)$ , while  $\Psi_{l,A}(\xi + 1)$  is strictly increasing in  $\xi$ .

Turning to (iii), we pick  $\xi \in (-1 - \frac{1}{l}, -1)$  and compute

$$\frac{d^2}{d\xi^2} \Delta_k[\Psi_{l,A}](\xi) = -Al^{-1-\xi} \log(l) (2(1+k)l^{3+\xi}(1+l+l\xi) + k \log(l)) < 0,$$

since  $1 + l + l\xi > 1 + l + l(-1 - \frac{1}{l}) = 0$  and  $l > 1$ . For the remaining claim (iv), we take  $\xi \in [-1, 0)$  and observe that  $\Psi_{l,A}(\xi - 1) > \kappa_{l,A}(\xi - 1)$ , while on the other hand  $\Psi_{l,A}(\xi) = \kappa_{l,A}(\xi)$  and  $\Psi_{l,A}(\xi + 1) = \kappa_{l,A}(\xi + 1)$ .  $\square$

At this point it is convenient to extend the definition (2.12) of  $d^*(a, k)$  by writing

$$d^*(a; l, A, k) = \frac{1}{(k-l)(1-\frac{1}{l})} \max_{s \in [1-\frac{a}{A}, 1]} \frac{-g(A(1-s); a)}{As}, \quad (6.6)$$

which reduces to (2.12) in the special case  $A = 1$  and  $l = \sqrt{k}$ , which maximizes the value of  $d^*$  when the other two parameters ( $a$  and  $k$ ) are fixed. The following lemma shows that  $\Psi_{l,A}$  can act as a sub-solution with negative speed when  $d > d^*(a; l, A, k)$ .

**Lemma 6.2.** *Assume that (Hg) holds and pick  $a \in (0, 1)$ ,  $A \in [a, 1)$ ,  $k > 1$  and  $l \in (1, k)$ . Then for any  $d > d^*(a; l, A, k)$  there exists  $\bar{c} < 0$  so that  $\mathcal{I}_{a,d,k}[\bar{c}, \Psi_{l,A}](\xi) \leq 0$  for all  $\xi \in \mathbb{R}$ .*

*Proof.* The condition  $d > d^*(a; l, A, k)$  ensures the existence of  $\varepsilon > 0$  such that

$$d = d^*(a; l, A, k) + \frac{\varepsilon}{(k-l)(1-\frac{1}{l})}. \quad (6.7)$$

Note that Lemma 6.1 allows us to define the positive constant

$$C := \inf_{\xi \in (-1-\frac{1}{l}, 0)} \Delta_k[\Psi_{l,A}](\xi) > 0, \quad (6.8)$$

enabling us to choose  $\bar{c} < 0$  in such a way that

$$\bar{c} > \max \left\{ -\frac{\varepsilon}{\log(l)}, -\frac{\varepsilon C}{A(k-l)(1-\frac{1}{l})l \log(l)} \right\}. \quad (6.9)$$

We now proceed to show that  $\mathcal{I}_{a,d,k}[\bar{c}, \Psi_{l,A}](\xi) \leq 0$  for all  $\xi \in \mathbb{R}$  by considering three separate cases.

**Case 1:** For  $\xi \leq -1 - \frac{1}{l}$ , we have  $\Psi'_{l,A}(\xi) = 0$  and  $\Delta_k[\Psi_{l,A}](\xi) \geq 0$  by items (i) and (ii) of Lemma 6.1. Using (Hg), we hence find

$$\begin{aligned} \mathcal{I}_{a,d,k}[\bar{c}, \Psi_{l,A}](\xi) &= -\bar{c}\Psi'_{l,A}(\xi) - d\Delta_k[\Psi_{l,A}](\xi) - g(\Psi_{l,A}(\xi); a) \\ &\leq -g(\Psi_{l,A}(\xi); a) < 0. \end{aligned}$$

**Case 2:** For  $\xi \in (-1 - \frac{1}{l}, 0]$ , we compute

$$\begin{aligned} \mathcal{I}_{a,d,k}[\bar{c}, \Psi_{l,A}](\xi) &= -\bar{c}\Psi'_{l,A}(\xi) - d\Delta_k[\Psi_{l,A}](\xi) - g(\Psi_{l,A}(\xi); a) \\ &\leq -\bar{c}\Psi'_{l,A}(\xi) - d\Delta_k[\Psi_{l,A}](\xi) \\ &\leq \frac{\varepsilon C}{A(k-l)(1-\frac{1}{l})l \log(l)} Al \log(l) - \left( d^*(a; l, A, k) + \frac{\varepsilon}{(k-l)(1-\frac{1}{l})} \right) C \\ &= -d^*(a; l, A, k)C < 0. \end{aligned}$$

Here the first inequality follows from (Hg), while the second one uses (6.9), (6.5), (6.6) and (6.8), respectively.

**Case 3:** For  $\xi > 0$ , we have  $\Psi_{l,A}(\xi) = \kappa_{l,A}(\xi)$  by (6.4) and  $\Delta_k[\Psi_{l,A}](\xi) = \Delta_k[\kappa_{l,A}](\xi)$  by item (v) of Lemma 6.1. We now use (6.9), (6.3) and (6.2) to compute

$$\begin{aligned} \mathcal{I}_{a,d,k}[\bar{c}, \Psi_{l,A}](\xi) &= -\bar{c}\Psi'_{l,A}(\xi) - d\Delta_k[\Psi_{l,A}](\xi) - g(\Psi_{l,A}(\xi); a) \\ &\leq \frac{\varepsilon}{\log(l)} Al^{-\xi} \log(l) - dAl^{-\xi}(k-l) \left(1 - \frac{1}{l}\right) - g(A(1-l^{-\xi}); a) \\ &= \varepsilon Al^{-\xi} - dAl^{-\xi}(k-l) \left(1 - \frac{1}{l}\right) - g(A(1-l^{-\xi}); a). \end{aligned}$$

Next, we use the substitution

$$x := l^{-\xi}, \quad x \in (0, 1)$$

together with (6.6) to obtain

$$\begin{aligned} \mathcal{I}_{a,d,k}[\bar{c}, \Psi_{l,A}](\xi) &\leq \varepsilon Ax - \left( d^*(a; l, A, k) + \frac{\varepsilon}{(k-l) \left(1 - \frac{1}{l}\right)} \right) Ax(k-l) \left(1 - \frac{1}{l}\right) - g(A(1-x); a), \\ &= x \left( - \max_{s \in [1 - \frac{a}{A}, 1]} \frac{-g(A(1-s); a)}{s} - \frac{g(A(1-x); a)}{x} \right). \end{aligned} \quad (6.10)$$

Now, if  $x \in [1 - \frac{a}{A}, 1)$ , then

$$\max_{s \in [1 - \frac{a}{A}, 1]} \frac{-g(A(1-s); a)}{s} \geq - \frac{g(A(1-x); a)}{x}$$

and if  $x \in (0, 1 - \frac{a}{A})$ , then  $-g(A(1-x); a) < 0$ . Either way, we deduce from (6.10) that

$$\mathcal{I}_{a,d,k}[\bar{c}, \Psi_{l,A}](\xi) \leq 0, \quad \xi > 0,$$

which completes the proof.  $\square$

*Proof of Theorem 2.5.* Substituting  $A(1-s) = 1-y$ , we find

$$d^*(a; l, A, k) = \frac{1}{(k-l) \left(1 - \frac{1}{l}\right)} \max_{s \in [1 - \frac{a}{A}, 1]} \frac{-g(A(1-s); a)}{As} = \frac{1}{(k-l) \left(1 - \frac{1}{l}\right)} \max_{y \in [1-a, 1]} \frac{-g(1-y; a)}{A-1+y}.$$

Clearly,  $d^*(a; l, A, k)$  is continuously decreasing with respect to  $A$  and

$$\lim_{A \rightarrow 1^-} d^*(a; l, A, k) = d^*(a; l, 1, k).$$

Consequently, whenever  $d > d^*(a; \sqrt{k}, 1, k)$ , there exists  $\bar{A} < 1$  (close to 1) so that  $d > d^*(a; \sqrt{k}, \bar{A}, k)$ . An application of Lemma 6.2 now concludes the proof.  $\square$

## 7 Cubic nonlinearity

The aim of this section is to prove Proposition 2.9, which explicitly describes the region  $\mathcal{D}^-$  for the standard cubic nonlinearity

$$g(v; a) = v(1-v)(v-a). \quad (7.1)$$

We achieve this by finding explicit expressions for the slope  $d^\circ$  defined in (2.14). The definition of  $d^\circ(A; a)$  directly depends on the convexity regions of our cubic nonlinearity. Namely, there exists a unique inflection point  $v_i = v_i(a)$  on the interval  $(0, 1)$  such that  $g$  is convex on  $(0, v_i)$  and concave on  $(v_i, 1)$ . A straightforward computation shows that

$$v_i(a) = \frac{a+1}{3}.$$

**Lemma 7.1.** *Let  $g$  be the standard cubic nonlinearity (7.1). Pick any  $a \in (0, 1)$  and  $A \in (v_i, 1)$ . Then the linear function*

$$v \mapsto d^\circ(k+1)(A-v) - g(A; a)$$

*touches the nonlinearity  $v \mapsto -g(v; a)$  tangentially at some touching point  $u_{tp}$ ; see Fig 5 (left). Moreover, we have*

$$u_{tp} = \frac{1}{2}(1+a-A) \in \left(\frac{a}{2}, v_i\right), \quad (7.2)$$

$$d^\circ(A; a) = \frac{-3A^2 + 2(a+1)A + (a-1)^2}{4(k+1)} > 0. \quad (7.3)$$

*Proof.* In order to find  $d^\circ(A; a)$  and the touching point  $u_{tp}$  for  $A \in (v_i, 1)$  we exploit the idea used by Keener in [15] for  $k = 1$  and match the coefficients of two cubic polynomials. In particular, we write

$$g(v; a) + d^\circ(k+1)(A-v) - g(A; a) = (v - u_{tp})^2(A-v). \quad (7.4)$$

The polynomial on the right-hand-side is always positive on  $[0, A]$ . Moreover, if we show that  $u_{tp} < A$ , then  $d^\circ(k+1)$  is indeed the smallest possible slope such that the line  $d^\circ(k+1)(A-v) - g(A; a)$  stays above the graph of  $-g$  for  $v \in [0, A]$ . However, this inequality follows easily from  $A > v_i$  which implies that  $u_{tp} < v_i < A$ .  $\square$

**Lemma 7.2.** *Pick  $a \in (0, \frac{1}{2})$  and  $A \in (a, v_i)$ . Then we have*

$$d^\circ(A; a) = \frac{g'(A; a)}{k+1}. \quad (7.5)$$

*Proof.* The choice  $a < \frac{1}{2}$  implies that the function  $-g$  is concave on  $(0, v_i)$ . This implies that the line with the smallest slope that stays above the graph of  $-g$  on the interval  $(0, A) \subset (0, v_i)$  is indeed given by  $d^\circ(k+1)(A-v) - g(A; a)$  for  $d^\circ = g'(A; a)/(k+1)$ .  $\square$

Recall the definition (2.15) and pick  $a \in (0, 1)$ . We denote by  $\mathcal{A}(a)$  the set of admissible parameters  $A$ , namely

$$A \in \mathcal{A}(a) \iff d^\circ(A; a) \leq \frac{g(A; a)}{A}. \quad (7.6)$$

On account of Lemmas 7.1 and 7.2, we have to separately consider the two cases  $A \in (a, v_i)$  and  $A \in (v_i, 1)$  in our study of  $d^\circ(A; a)$ . We therefore define two subsets of  $\mathcal{A}(a)$ , namely

$$\mathcal{A}_1(a) = (a, v_i) \cap \mathcal{A}(a), \quad \mathcal{A}_2(a) = [v_i, 1) \cap \mathcal{A}(a).$$

A key point in our analysis is that the contribution from the parameters  $A \in (a, v_i)$  can be safely neglected. In particular, we have the following result.

**Lemma 7.3.** *Let  $g$  be the standard cubic nonlinearity (7.1). Then we have the identities*

$$\min_{A \in \mathcal{A}(a)} d^\circ(A; a) = \min_{A \in \mathcal{A}_2(a)} d^\circ(A; a), \quad (7.7)$$

$$\max_{A \in \mathcal{A}(a)} \frac{g(A; a)}{A} = \max_{A \in \mathcal{A}_2(a)} \frac{g(A; a)}{A}. \quad (7.8)$$

*Proof.* See §7.1.  $\square$

In the following lemma we further characterize the set  $\mathcal{A}_2(a)$ . In particular, we show that there exists an upper bound on  $a$  for which  $\mathcal{A}_2(a)$  is not an empty set.

**Lemma 7.4.** *Let  $g$  be the standard cubic nonlinearity (7.1). Pick any parameter  $a \in (0, 1)$  and recall the value  $a_*^-(k)$  defined by (2.20). Then the following claims hold.*

(i) *If  $a > a_*^-(k)$  then*

$$\mathcal{A}_2(a) = \emptyset.$$

(ii) If  $a \leq a_*^-(k)$  then

$$\mathcal{A}_2(a) = [v_i, 1) \cap [A_2^-(a), A_2^+(a)],$$

where  $A_2^-(a)$  and  $A_2^+(a)$  are defined by

$$A_2^-(a) = \frac{(1+a)(1+2k) - 2\sqrt{k^2(a-1)^2 - ka}}{4k+1},$$

$$A_2^+(a) = \frac{(1+a)(1+2k) + 2\sqrt{k^2(a-1)^2 - ka}}{4k+1}.$$

Moreover, we have the inequalities

$$A_2^+(a) \geq \frac{a+1}{2}, \quad A_2^+(a) \in (1-a, 1). \quad (7.9)$$

*Proof.* Pick  $A \in [v_i, 1)$ . By Lemma 7.1, we have  $A \in \mathcal{A}_2(a)$  if and only if

$$\frac{-3A^2 + 2(a+1)A + (a-1)^2}{4(k+1)} \leq (1-A)(A-a). \quad (7.10)$$

This quadratic inequality has solutions if and only if  $A \in [A_2^-(a), A_2^+(a)]$ , which are well defined for

$$k^2(a-1)^2 - ka \geq 0,$$

which is equivalent to  $a \leq a_*^-(k)$ . On the other hand, for  $a > a_*^-(k)$  there is no solution to (7.10), establishing (i).

The inequality  $A_2^+(a) > (1+a)/2$  follows directly from

$$A_2^+(a) \geq \frac{(1+a)(1+2k)}{4k+1} = \frac{(1+a)}{2} + \frac{(1+a)}{2(4k+1)} > \frac{(1+a)}{2}.$$

To show  $A_2^+(a) > 1-a$ , we write

$$A_2^+(a) - (1-a) = 2 \frac{a(1+3k) - k + \sqrt{k^2(1-a)^2 - ka}}{1+4k}.$$

For  $a \geq k/(1+3k)$  the numerator is immediately positive. To examine the case  $a < k/(1+3k)$  we define the quadratic expression  $\mathcal{Q}_1(a, k)$  by

$$\mathcal{Q}_1(a, k) = k^2(1-a)^2 - ka - (a+3ka-k)^2 = a(k+4k^2 - (1+6k+8k^2)a).$$

This is strictly positive for  $0 < a \leq \frac{k}{1+3k}$ , since  $\mathcal{Q}_1(0, k) = 0$  and

$$\mathcal{Q}_1\left(\frac{k}{1+3k}, k\right) = \frac{k}{1+3k} \frac{k^2(1+4k)}{1+3k} = \frac{k^3(1+4k)}{(1+3k)^2} > 0.$$

To establish our final inequality  $A_2^+(a) < 1$ , we note that

$$1 - A_2^+(a) = \frac{2k - (1+2k)a - 2\sqrt{k^2(1-a)^2 - ka}}{1+4k}. \quad (7.11)$$

Upon writing

$$\mathcal{Q}_2(a, k) = (2k - (1+2k)a)^2 - 4(k^2(1-a)^2 - ka) = (1+4k)a^2,$$

we see that (7.11) is indeed strictly positive.  $\square$

**Lemma 7.5.** *Let  $g$  be the standard cubic nonlinearity (7.1). Pick  $k > 0$  together with  $a \in (0, a_*^-(k))$  and recall the constant  $a_1^-(k)$  defined by (2.20). Then we have*

$$\max_{A \in \mathcal{A}_2(a)} \frac{g(A; a)}{A} = \begin{cases} \frac{(1-a)^2}{4}, & \text{if } a \in (0, a_1^-(k)], \\ \frac{g(A_2^-(a); a)}{A_2^-(a)}, & \text{if } a \in [a_1^-(k), a_*^-(k)]. \end{cases}$$

*Proof.* Let us first define  $A_{\max} = \frac{a+1}{2}$ . A standard analysis shows that

$$\max_{A \in (0,1)} \frac{g(A; a)}{A} = \frac{g(A_{\max}; a)}{A_{\max}}.$$

By Lemma 7.4 we have

$$\max_{A \in \mathcal{A}_2(a)} \frac{g(A; a)}{A} = \begin{cases} \frac{g(A_{\max}; a)}{A_{\max}}, & A_2^-(a) \leq A_{\max}, \\ \frac{g(A_2^-(a); a)}{A_2^-(a)}, & A_2^-(a) \geq A_{\max}. \end{cases}$$

We claim that for  $a \in (0, 1)$  we have

$$A_2^-(a) \leq A_{\max}(a) \iff a \in (0, a_1^-(k)). \quad (7.12)$$

Indeed, the inequality on the left can be written as

$$\frac{(1+a)(1+2k) - 2\sqrt{k^2(a-1)^2 - ka}}{4k+1} \leq \frac{1+a}{2},$$

which reduces to

$$a^2(4k-1) - 2a(4k+1) + 4k-1 \geq 0. \quad (7.13)$$

If  $k > 1/4$  then this expression is positive for

$$a \leq 1 - \frac{4\sqrt{k}-2}{4k-1} = 1 - \frac{2}{2\sqrt{k}+1} \quad \text{and} \quad a \geq 1 + \frac{2}{2\sqrt{k}-1}.$$

We recognize that the first value is exactly equal to  $a_1^-(k)$ , while the second value is greater than 1 and therefore not of interest. For  $k \leq 1/4$  there is no solution of (7.13) in the set of positive numbers.  $\square$

**Lemma 7.6.** *Let  $g$  be the standard cubic nonlinearity (7.1) and pick any  $a \in (0, a_*^-(k))$ . Then we have*

$$\min_{A \in \mathcal{A}_2^+(a)} d^\circ(A; a) = \frac{g(A_2^+(a); a)}{A_2^+(a)}.$$

*Proof.* The graph of  $d^\circ(A; a)$  is a downwards parabola, positive on some superset of  $(0, 1)$ , with the maximum at  $A = v_i \leq A_2^+(a) < 1$ . Therefore, the minimum is attained at the right boundary  $A_2^+(a)$ .  $\square$

*Proof of Proposition 2.9.* Direct computation yields

$$\begin{aligned} \frac{g(A_2^-(a); a)}{A_2^-(a)} &= \frac{2a^2k - a + 2k + 2(a+1)\sqrt{k}\sqrt{ka^2 - a(2k+1) + k}}{(4k+1)^2}, \\ \frac{g(A_2^+(a); a)}{A_2^+(a)} &= \frac{2a^2k - a + 2k - 2(a+1)\sqrt{k}\sqrt{ka^2 - a(2k+1) + k}}{(4k+1)^2}. \end{aligned}$$

Applying Lemmas 7.3, 7.5 and 7.6 now guarantees that the upper and lower boundary of the set  $\mathcal{D}^-$  are given by  $d_{\max}$  and  $d_{\min}$ . The fact that the cubic nonlinearity satisfies (Hg1) ensures that the whole set  $\mathcal{D}^-$  is given as the area between these curves, establishing (iii). Items (i) and (ii) follow directly from the construction of  $d_{\max}$  and  $d_{\min}$ .  $\square$

## 7.1 Proof of Lemma 7.3

In this section we complete our analysis of the cubic nonlinearity by establishing Lemma 7.3. In addition to the points  $a_*^-(k)$  and  $a_1^-(k)$  defined by (2.20), we introduce a third value that plays an important role in this section, namely

$$a_2(k) := \min \left\{ 0, 1 - \frac{2\sqrt{k+4}}{\sqrt{k+4} + 3\sqrt{k}} \right\}. \quad (7.14)$$

In the following lemma we show that these three points are always ordered, irrespective of  $k > 0$ .

**Lemma 7.7.** *For every  $k > 0$  we have the ordering*

$$a_2(k) \leq a_1^-(k) < a_*^-(k). \quad (7.15)$$

*Proof.* Our first observation is that for  $k > 0$  we have

$$\begin{aligned} a_1^-(k) > 0 &\iff k > \frac{1}{4}, \\ a_2(k) > 0 &\iff k > \frac{1}{2}, \\ a_*^-(k) > 0 &\iff k > 0. \end{aligned}$$

Therefore, for  $k \leq \frac{1}{2}$  the ordering  $a_2(k) \leq a_1^-(k)$  trivially holds. For  $k > \frac{1}{2}$ , the inequality  $a_2(k) \leq a_1^-(k)$  is equivalent to

$$\frac{1}{2\sqrt{k} + 1} \leq \frac{\sqrt{k+4}}{\sqrt{k+4} + 3\sqrt{k}},$$

which is in turn equivalent to

$$\sqrt{k} (2\sqrt{k+4} - 3) \geq 0.$$

This holds for all  $k > 0$ . To show  $a_1^-(k) \leq a_*^-(k)$  we apply the bound  $\sqrt{4k+1} \geq 2\sqrt{k}$  to the denominator of  $a_*^-(k)$ . This concludes the proof.  $\square$

**Lemma 7.8.** *Let  $g$  be the standard cubic nonlinearity (7.1). Pick  $k > 0$  and  $a \in (0, \frac{1}{2})$ . Then we have*

$$\mathcal{A}_1(a) \neq \emptyset \iff a \in (0, a_2(k)).$$

*Proof.* In view of Lemma 7.2, we have  $d^\circ(A; a) \leq g(A; a)/A$  if and only if

$$\frac{g'(A; a)}{k+1} \leq \frac{g(A; a)}{A}, \quad (7.16)$$

which can be rewritten as

$$f(A; a) := A^2(k-2) + A(1-k)(a+1) + ka \leq 0.$$

To examine this quadratic function, we first note that  $f(a; a) = a(1-a) > 0$  and  $f(1; a) = a-1 < 0$ . By showing that

$$\bar{f}(a) := f(v_i; a) = f\left(\frac{a+1}{3}; a\right) > 0 \iff a > a_2(k),$$

it follows that  $f$  must also be positive on  $(a, v_i)$ . Consequently, there exists no  $A \in (a, v_i)$  such that  $\bar{f}(A) \leq 0$ . To establish this claim, we compute

$$\bar{f}(a) = \frac{1}{9} ((1-2k)a^2 + (2+5k)a + 1 - 2k). \quad (7.17)$$

For  $k > 1/2$ , the graph of the mapping  $a \mapsto \bar{f}(a)$  is a downward orientated parabola with two roots, the smaller of which is given exactly by  $a_2(k)$ . Moreover, we can directly check that the expression  $\bar{f}(1/2)$  is equal to  $0.25 > 0$ . Therefore, for all  $a \in (a_2(k), 1/2)$  we have  $\bar{f}(a) > 0$ . For  $k \leq 1/2$ , all roots of  $a \mapsto \bar{f}(a)$  are nonpositive, which implies that  $\mathcal{A}_1(a)$  is an empty set for all  $a \in (0, \frac{1}{2})$ .  $\square$



**Lemma 7.9.** *Let  $g$  be the standard cubic nonlinearity (7.1). Pick any  $a \in (0, a_*^-(k))$ . Then we have*

$$\max_{A \in \mathcal{A}_1(a)} \frac{g(A; a)}{A} \leq \max_{A \in \mathcal{A}_2(a)} \frac{g(A; a)}{A}.$$

*Proof.* If  $a > a_2(k)$  the claim trivially holds since  $\mathcal{A}_1(a) = \emptyset$ . If  $a \leq a_2(k)$  then we automatically have  $a \leq a_1^-(k)$  due to Lemma 7.9. By Lemma 7.5 the maximum of  $g(A; a)/A$  is attained on  $(0, a_1^-(k)]$  as  $A_{\max}$  belongs to  $\mathcal{A}_2(a)$ . Therefore, the contribution from the values of  $A \in \mathcal{A}_1(a)$  cannot exceed this maximum.  $\square$

**Lemma 7.10.** *Let  $g$  be the standard cubic nonlinearity (7.1). Pick any  $a \in (0, a_*^-(k))$ . Then we have*

$$\min_{A \in \mathcal{A}_1(a)} d^\circ(A; a) \geq \min_{A \in \mathcal{A}_2(a)} d^\circ(A; a).$$

*Proof.* If  $a \geq a_2(k)$  the claim trivially holds since  $\mathcal{A}_1(a) = \emptyset$ . We therefore assume  $a \in (0, a_2(k))$  and recall from Lemma 7.6 that

$$\min_{A \in \mathcal{A}_2(a)} d^\circ(A; a) = \frac{g(A_2^+(a))}{A_2^+(a)}.$$

By Lemma 7.4 we also know that  $A_2^+(a) > 1 - a$ , which in turn gives

$$u_{tp}(A_2^+(a)) < a. \quad (7.18)$$

Assume now to the contrary that there exists  $A \in \mathcal{A}_1(a) \subset (v_i, a)$  for which

$$\frac{g(A_2^+(a); a)}{A_2^+(a)} > \frac{g'(A; a)}{k+1}. \quad (7.19)$$

Since  $-g$  is concave on  $(v_i, a)$  the linear map  $g'(A; a)(A - v) - g(A; a)$  crosses the  $v$ -axis at some point  $\tilde{A} > a$ . However, (7.18) automatically implies that  $d^\circ(A_2^+(a); a) \leq g'(A; a)/(k+1)$ , which clearly contradicts (7.19) and hence establishes our claim.  $\square$

*Proof of Lemma 7.3.* The claim follows directly from Lemmas 7.9 and 7.10.  $\square$

## 8 Spatial chaos

To prove Proposition 2.4, we follow the outline from [15] and adapt the Moser theorem from [20]. We first note that the solutions of the MFDE (2.4) with  $c = 0$  are equivalent to steady-state solutions of (2.1), i.e., sequences  $(u_i)_{i \in \mathbb{Z}}$  that satisfy the difference equation

$$d(u_{i-1} - (k+1)u_i + ku_{i+1}) + g(u_i; a) = 0. \quad (8.1)$$

To find a solution to (8.1), we introduce a new sequence  $(v_i)_{i \in \mathbb{Z}}$  by setting  $v_i := u_{i-1}$ . This allows to rewrite (8.1) as the two-dimensional recursion relation

$$\begin{cases} v_{i+1} &= u_i, \\ u_{i+1} &= \frac{k+1}{k}u_i - \frac{v_i}{k} - \frac{g(u_i; a)}{kd}, \end{cases} \quad (8.2)$$

for  $i \in \mathbb{Z}$ . Writing  $\phi : \mathbb{R}^2 \rightarrow \mathbb{R}^2$  for the map

$$\phi(u, v) := \left( \frac{k+1}{k}u - \frac{1}{k}v - \frac{g(u; a)}{kd}, u \right), \quad (8.3)$$

we notice that solving (8.2) is equivalent to constructing a sequence  $(u_i, v_i)_{i \in \mathbb{Z}}$  in  $\mathbb{R}^2$  that has

$$\phi(u_i, v_i) = (u_{i+1}, v_{i+1}). \quad (8.4)$$

The inverse of the mapping  $\phi$  is given by

$$\phi^{-1}(\tilde{u}, \tilde{v}) = \left( \tilde{v}, (k+1)\tilde{v} - k\tilde{u} - \frac{1}{d}g(\tilde{v}; a) \right) \quad (8.5)$$

and a straightforward calculation shows that  $\phi$  and  $\phi^{-1}$  are further related by the identity

$$\phi^{-1} = R_k \phi R_k,$$

where  $R_k$  is given by

$$R_k = \begin{pmatrix} 0 & 1 \\ k & 0 \end{pmatrix}.$$

In the special case  $k = 1$ , this matrix represent reflection through the line  $v = u$ .

## 8.1 The Moser theorem

We first define a few notions that we use throughout this section. We call a curve  $v = v(u)$  a *horizontal curve* if  $0 \leq v(u) \leq 1$  for  $0 \leq u \leq 1$ . Analogously, we call a curve  $u = u(v)$  a *vertical curve* if  $0 \leq u(v) \leq 1$  for  $0 \leq v \leq 1$ . For two disjoint horizontal curves  $0 \leq v_1(u) < v_2(u) \leq 1$  we call the set

$$U = \{(u, v) : 0 \leq u \leq 1 : v_1(u) \leq v \leq v_2(u)\}$$

a *horizontal strip*. Similarly, we define a *vertical strip* as an area  $V$  lying between disjoint vertical curves  $0 \leq u_1(v) < u_2(v) \leq 1$ , namely

$$V = \{(u, v) : 0 \leq v \leq 1 : u_1(v) \leq u \leq u_2(v)\}.$$

We also introduce the space  $\mathcal{S}$  containing all bi-infinite sequences with elements in  $\{0, 1\}$ , i.e.,

$$\mathcal{S} := \{(\dots, s_{-2}, s_{-1}, s_0, s_1, s_2, \dots) : s_i \in \{0, 1\}\}.$$

This space  $\mathcal{S}$  when endowed with an appropriate topology makes a topological space [20], on which we define the forward shift  $\sigma : \mathcal{S} \rightarrow \mathcal{S}$  by

$$[\sigma(s)]_i = s_{i+1}.$$

**Theorem 8.1.** [20, Moser] *Suppose for  $n \in \{0, 1\}$  that  $U_n, V_n$  are disjoint horizontal and vertical, respectively, strips in  $Q := [0, 1]^2$  that additionally satisfy*

(i)  $\phi(V_n) = U_n, n \in \{0, 1\}$ .

(ii) *The vertical boundaries of  $V_n$  are mapped to vertical boundaries of  $U_n$  and the horizontal boundaries of  $V_n$  are mapped to horizontal boundaries of  $U_n$ .*

*Then there exists a function  $\tau : \mathcal{S} \mapsto \mathcal{Q}$  such that*

$$\phi\tau = \tau\sigma.$$

*In addition, the function  $\tau$  satisfies*

$$\phi^i \tau(s) \in U_{s_i}, \quad s \in \mathcal{S}, \quad i \in \mathbb{Z}.$$

Stated informally, we say that  $\phi$  possesses the shift  $\sigma$  on sequences of elements of  $\{0, 1\}$  as a subsystem. The main consequence of the Moser theorem is that for every sequence  $s \in \mathcal{S}$  we can find a sequence  $(u_i, v_i)_{i \in \mathbb{Z}}$  satisfying (8.4) with  $(u_i, v_i) \in U_{s_i}$  for every  $i \in \mathbb{Z}$ . To achieve this, we simply set  $(u_0, v_0) := \tau(s)$  and  $(u_i, v_i) := \phi^i(u_0, v_0)$ .

**Construction of horizontal and vertical strips** Let us define a function  $h$  that acts as

$$h(v; a, d) = (k+1)v - \frac{1}{d}g(v; a). \quad (8.6)$$

To construct the strips  $U_n$  and  $V_n$ , for  $n = 0, 1$ , we need to ensure that the parameter  $d$  is small enough so that the following assumption holds.

(Hd) There exist points  $y_0$  and  $y_1$ , satisfying  $0 < y_0 < a$  and  $a < y_1 < 1$  such that

$$\begin{aligned} h(y_0; a, d) &> k+1, \\ h(y_1; a, d) &< 0, \\ h'(v; a, d) &> 0, \quad v \in (0, y_0) \cup (y_1, 1). \end{aligned}$$

**Lemma 8.2.** *Assume that conditions (Hg) and (Hd) hold. Then there exist horizontal strips  $U_0, U_1$ , and vertical strips  $V_0, V_1$  that satisfy the assumptions of Theorem 8.1.*

*Proof of Proposition 2.4.* It suffices to show that the function  $h$  defined by (8.6) satisfies condition (Hd) for all sufficiently small  $d > 0$ . Indeed, we can then combine the Moser Theorem 8.1 and Lemma 8.2 to obtain the desired conclusion.

On the interval  $(0, a)$  we have

$$h(v; a, d) - (k+1) = (k+1)(v-1) - \frac{1}{d}g(v; a) \geq -(k+1) - \frac{1}{d}g(v; a).$$

We now choose  $\delta > 0$  in such a way that the function  $v \mapsto g(v; a)$  is strictly negative and decreasing on  $(0, \delta)$ . By choosing  $d$  small enough we can therefore achieve  $h(\delta; a, d) - (k+1) > 0$ . This shows that we can choose  $y_0 = \delta$ . The point  $y_1$  can be found analogously.  $\square$

**Lemma 8.3.** *Assume that conditions (Hg) and (Hd) hold. Then there exist six points  $(x_i)_{i=1}^3$  and  $(z_i)_{i=0}^2$  that satisfy the identities*

$$\begin{aligned} h(x_1; a, d) &= 1, & h(x_2; a, d) &= k, & h(x_3; a, d) &= k+1, \\ h(z_0; a, d) &= 0, & h(z_1; a, d) &= 1, & h(z_2; a, d) &= k, \end{aligned}$$

together with the identities

$$0 < x_1 < x_2 < x_3 < y_0 < a < y_1 < z_0 < z_1 < z_2 < 1.$$

*Proof.* The existence of  $x_1, x_2$  and  $x_3$  follow directly from assumption (Hd). In addition, we have  $h(1; a, d) = k+1$  and  $h(y_1; a, d) < 0$ . Again, the monotonicity assumption ensures that we can find points  $z_0 < z_1 < z_2 < 1$  that satisfy the claim.  $\square$

*Proof of Lemma 8.2.* We define the curves  $u_1$  and  $u_2$  by writing

$$\begin{aligned} u_1 &:= \left\{ (u, v) \in \mathbb{R}^2 : 0 \leq u \leq x_1, v = (k+1)u - \frac{1}{d}g(u; a) \right\} = \phi^{-1}\{(0, \tilde{v}) : 0 \leq \tilde{v} \leq x_1\}, \\ u_2 &:= \left\{ (u, v) \in \mathbb{R}^2 : x_2 \leq u \leq x_3, v = (k+1)u - k - \frac{1}{d}g(u; a) \right\} = \phi^{-1}\{(1, \tilde{v}) : x_2 \leq \tilde{v} \leq x_3\}. \end{aligned}$$

Using the definition of the points  $x_1, x_2$  and  $x_3$ , we see that the curve  $u_1$  connects the points  $(0, 0)$  and  $(x_1, 1)$ , while the curve  $u_2$  connects the points  $(x_2, 0)$  and  $(x_3, 1)$ . Due to the monotonicity of the mapping  $u \mapsto (k+1)u - \frac{1}{d}g(u; a)$  on  $[0, y_0]$ , both of these curves can be represented as graphs  $u_1(v)$  and  $u_2(v)$  for  $v \in [0, 1]$ . This proves that these are indeed vertical curves. We now define the set  $V_0$  as the area lying between those two curves, and we set  $U_0 := \phi(V_0)$ .

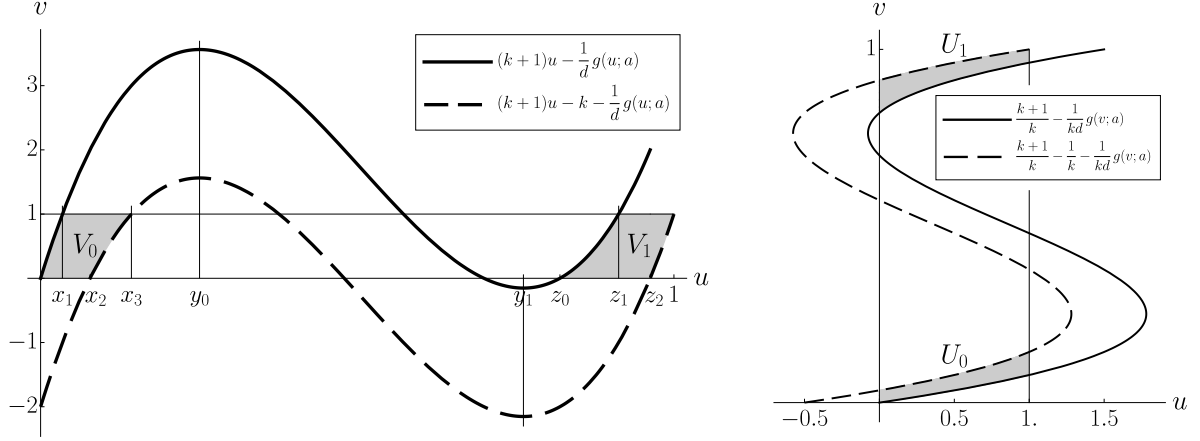


Figure 8: The sets  $V_n$ ,  $U_n$ ,  $n = 0, 1$  for  $k = 2$ ,  $d = 0.014$  and the cubic nonlinearity  $g(u; a) = u(1-u)(u-a)$  with  $a = 0.52$ .

It remains to show that  $U_0$  is a horizontal strip. The horizontal boundaries of  $V_0$ , characterized by  $\{(u, 0) : 0 \leq u \leq x_2\}$  and  $\{(u, 1) : x_1 \leq u \leq x_3\}$ , respectively, are mapped by  $\phi$  to the curves

$$v_1 := \left\{ \left( \frac{k+1}{k}u - \frac{g(u; a)}{kd}, u \right) : 0 \leq u \leq x_2 \right\},$$

$$v_2 := \left\{ \left( \frac{k+1}{k}u - \frac{1}{k} - \frac{g(u; a)}{kd}, u \right) : x_1 \leq u \leq x_3 \right\}.$$

The curve  $v_1$  connects the point  $(0, 0)$  with  $(1, x_2)$  whereas the curve  $v_2$  connects the point  $(0, x_1)$  with  $(1, x_3)$  and both of these curves are monotonically increasing, implying that they are horizontal strips.

Finally, the left vertical boundary  $u_1$  of  $V_0$  is by definition mapped to the set  $\{(0, \tilde{v}) : 0 \leq \tilde{v} \leq x_1\}$ , while the right vertical boundary  $u_2$  of  $V_0$  is mapped to the set  $\{(1, \tilde{v}) : x_2 \leq \tilde{v} \leq x_3\}$ . This shows that  $U_0$  is indeed a horizontal strip, with  $V_0$  and  $U_0$  satisfying item (ii).

To construct the set  $V_1$ , we define the curves  $u_3$  and  $u_4$  by writing

$$u_3 := \left\{ (u, v) \in \mathbb{R}^2 : z_0 \leq u \leq z_1, v = (k+1)u - \frac{1}{d}g(u; a) \right\} = \phi^{-1}\{(0, \tilde{v}) : z_0 \leq \tilde{v} \leq z_1\},$$

$$u_4 := \left\{ (u, v) \in \mathbb{R}^2 : z_2 \leq u \leq 1, v = (k+1)u - k - \frac{1}{d}g(u; a) \right\} = \phi^{-1}\{(1, \tilde{v}) : z_2 \leq \tilde{v} \leq 1\}.$$

Straightforward checks show that the curve  $u_3$  connects the points  $(z_0, 0)$  and  $(z_1, 1)$ , while the curve  $u_4$  connects the points  $(z_2, 0)$  and  $(1, 1)$ . The map

$$u \mapsto (k+1)u - \frac{1}{d}g(u; a)$$

is increasing on  $[y_1, 1]$  so both of these curves can be represented as graphs  $u_3(v)$  and  $u_4(v)$  for  $v \in [0, 1]$ . We define the set  $V_1$  as the area lying between these two curves and we set  $U_1 := \phi(V_1)$ .

The function  $\phi$  maps the horizontal boundaries of  $V_1$ , characterized by the sets

$$\{(u, 0) : z_0 \leq u \leq z_2\} \text{ and } \{(u, 1) : z_1 \leq u \leq 1\},$$

to the curves

$$v_3 := \left\{ \left( \frac{k+1}{k}u - \frac{g(u; a)}{kd}, u \right) : z_0 \leq u \leq z_2 \right\},$$

$$v_4 := \left\{ \left( \frac{k+1}{k}u - \frac{1}{k} - \frac{g(u; a)}{kd}, u \right) : z_1 \leq u \leq 1 \right\}.$$

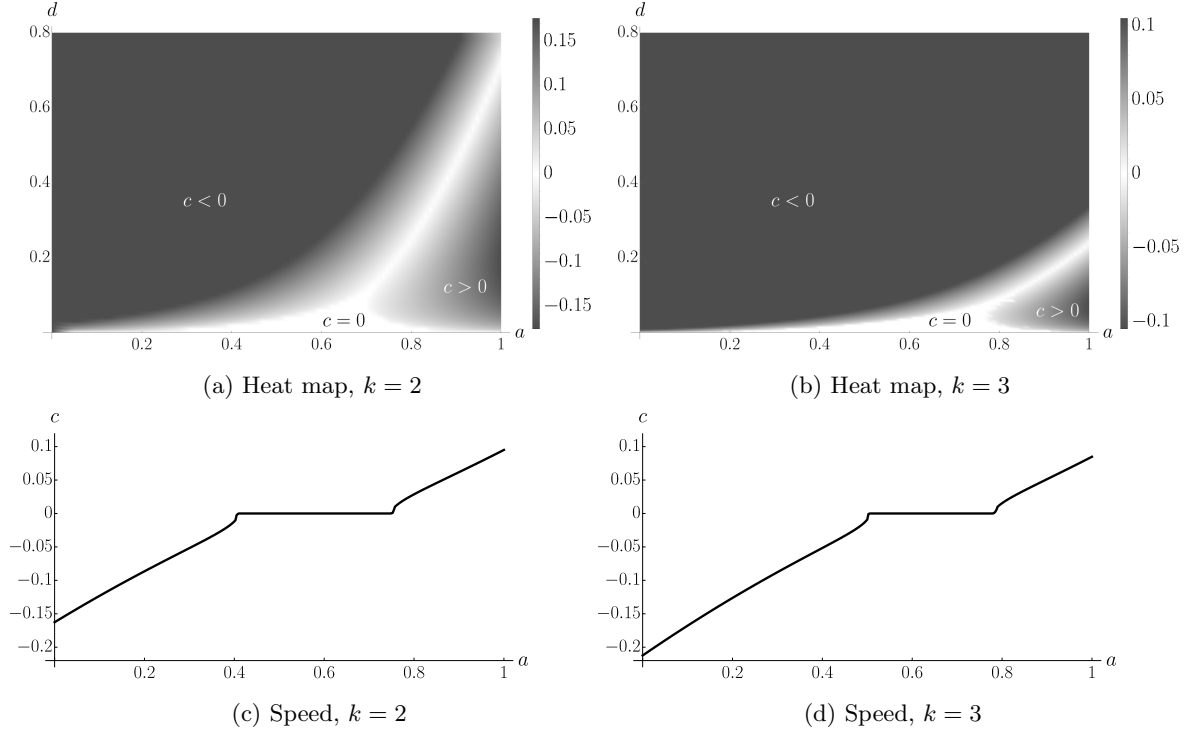


Figure 9: The dependence of wave speed  $c$  on the detuning parameter  $a$ , studied in Example 9.1 for  $k = 2$  (left panels) and  $k = 3$  (right panels). The top panels show the heat maps, the darker the color the higher the value of  $|c|$ . The bottom panels then show the speed for fixed  $d = 0.025$ .

The curve  $v_3$  connects the point  $(0, z_0)$  with  $(1, z_2)$  and curve  $v_4$  connects the point  $(0, z_1)$  with  $(1, 1)$ . Both of these curves are monotonically increasing.

As before, the left boundary  $u_3$  of  $V_1$  is mapped to  $\{(0, \tilde{v}) : z_0 \leq \tilde{v} \leq z_2\}$ , while the right boundary  $u_4$  of  $V_1$  is mapped to the set  $\{(1, \tilde{v}) : z_2 \leq \tilde{v} \leq 1\}$ . This finally proves that  $U_1$  is a horizontal strip, with  $V_1$  and  $U_1$  satisfying item (ii).  $\square$

In our final result we give the explicit formula for the curve  $d_0(a, k)$  for the standard cubic linearity (1.2).

**Lemma 8.4.** *Consider the setting of Proposition 2.4, let  $g$  be the standard cubic nonlinearity and define the function  $d_0$  by (2.19). Then for any  $0 < d < d_0(a, k)$  condition (Hd) holds.*

*Proof.* One can check that for  $d > 0$  the quadratic inequalities

$$\begin{aligned} d(k+1)(v-1) - v(1-v)(v-a) &> 0, \\ d(k+1)v - v(1-v)(v-a) &< 0 \end{aligned}$$

have a solution in the set of real numbers if and only if  $0 < d < d_0(a, k)$ .  $\square$

## 9 Numerical examples

In this final section we showcase two results of our numerical experiments. In the first example we fix the diffusion parameter  $d$ , the branching parameter  $k$  and study the dependence of the wave speed  $c$  on the detuning parameter  $a$ .

**Example 9.1.** (Propagation direction) In order to validate our theoretical findings for the standard cubic nonlinearity (1.2), we numerically solved the MFDE (2.4) on a domain  $[-L, L]$  for some large

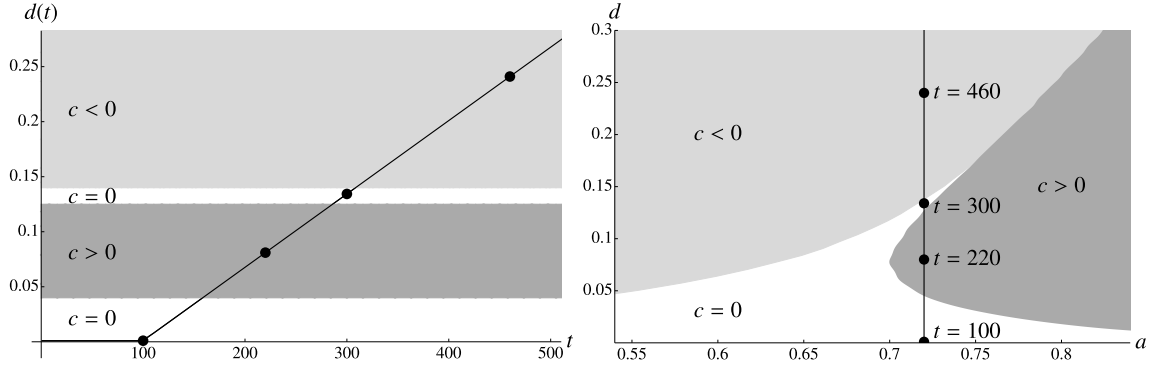


Figure 10: Illustration of the diffusion-driven propagation reversal discussed in Ex. 9.2. The nonconstant time-dependent diffusion  $d(t)$  given by (9.4) (left) and its trajectory through the  $(a, d)$  plane (right). The profiles in highlighted time entries  $t = 100, 220, 300$  and  $460$  are visualised in Fig. 11.

$L \gg 1$  with boundary conditions  $\Phi(-L) = 0, \Phi(L) = 1$ . For fixed  $(a, d) \in \mathcal{H}$ , we divided our domain into  $N_L \gg 1$  segments. Upon writing  $\Delta x = 2L/N_L$  we have  $N_L$  unknown variables - a speed  $c$  and  $N_L - 1$  spatial points

$$(\Phi_1, \dots, \Phi_{N_L-1}),$$

where each point  $\Phi_i$  approximates the value of  $\Phi(-L + i\Delta x)$ . It is important to note that  $N_L$  is chosen in such a manner that  $1/\Delta x = I_0 \in \mathbb{N}$ .

Moreover, we discretized the first derivatives in (2.4) by the fourth order central difference scheme. The complete discretization scheme then takes the form

$$0 = -\frac{c(8\Phi_{i+1} - 8\Phi_{i-1} - \Phi_{i+2} + \Phi_{i-2})}{12\Delta x} - d(k\Phi_{i+I_0} - (k+1)\Phi_i + \Phi_{i-I_0}) - g(\Phi_i; a) \quad (9.1)$$

for  $i = 1, \dots, N_L-1$ , to which we also add the boundary conditions  $\Phi_i = 0$  for all  $i \leq 0$  and  $\Phi_i = 0$  for all  $i \geq L$ . Adding the requirement

$$\Phi_{\lfloor \frac{N_L}{2} \rfloor} - \frac{1}{2} = 0, \quad (9.2)$$

to compensate for the shift-invariance, we rewrite this problem in the compact form as

$$F(c, \Phi_1, \dots, \Phi_{N_L-2}, \Phi_{N_L-1}) = 0, \quad (9.3)$$

where the function  $F : \mathbb{R}^{N_L} \rightarrow \mathbb{R}^{N_L}$  is derived from (9.1)-(9.2).

To this fixed point scheme we applied a nonlinear fixed-point solver using the Python programming language. We present our results in Fig. 9 using a colormap representation, i.e., to each value of the numerical speed  $c$  we assign a color. The darker the color the more distinct it is from zero.

Since numerical computations never provide exact values, it is not straightforward to determine when the speed of the wave is exactly equal to 0. Nevertheless, as the value of  $a$  increases from 0 to 1, keeping  $d$  fixed, one can observe that at some  $a = a_-$  a harsh jump occurs between the values  $|c| \gg 0$ , and  $c \approx 0$ . That is, the absolute value of the speed does not follow a smooth path but suddenly drops from values of the order  $10^{-2}$  to values of the order  $10^{-6}$  or even lower. Similarly, for some  $a = a_+$  the numerical speed suddenly rises from the low-order values back to the smooth trajectory. In view of the fact that  $c$  is a smooth, monotonic function with respect to the detuning parameter  $a$  whenever  $c \neq 0$ , we simply set  $c = 0$  in this region  $[a_-, a_+]$ . In Fig. 9, the numerical pinning region is depicted in white. We observe that the ‘cone’ in which  $c = 0$  becomes smaller as we increase  $k$ , which is in line with our theoretical results.

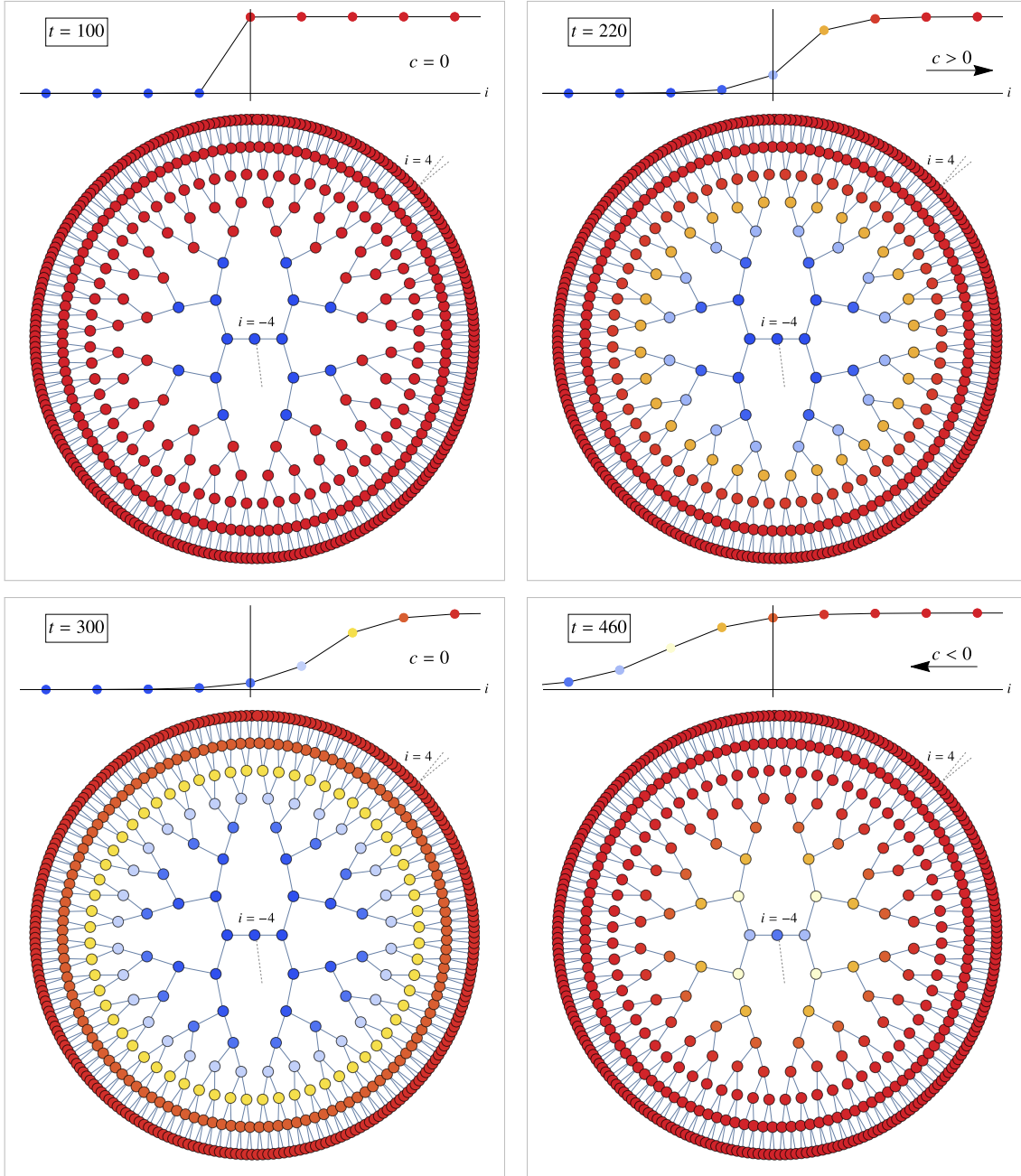


Figure 11: Illustration of the diffusion-driven propagation reversal discussed in Ex. 9.2. The top panels in each frame display the solutions  $u_i(t)$  of (9.5) at  $t = 100, 220, 300$  and  $460$ , see Fig. 10. The bottom panels in each frame depict the corresponding solutions of equation (1.4) on the binary tree  $\mathcal{T}_2$ . Only the layers with  $i = -4, -3, \dots, 3, 4$  are visualised. To see this figure in color, please go online.

In the second numerical experiment we highlight the phenomenon of the diffusion-driven propagation reversal. For this purpose vary the diffusion parameter  $d$  and fix the branching parameter  $k$  and the detuning parameter  $a \approx 1$ . This allows us to illustrate the diffusion-driven propagation reversal.

**Example 9.2** (Propagation reversal). In this example we illustrate the diffusion-driven propagation

reversal. Let the non-constant-diffusion be given by

$$d(t) = \begin{cases} .001 & t \leq 100, \\ .001 + \frac{1}{1500}(t - 100) & t > 100, \end{cases} \quad (9.4)$$

illustrated in the left panel of Fig. 10. We consider the bistable differential equation (1.1) on the binary tree  $\mathcal{T}_2$

$$\begin{cases} \dot{u}_i(t) = d(t) (2u_{i+1}(t) - 3u_i(t) + u_{i-1}(t)) + g(u_i(t); .72) \\ u_i(0) = \begin{cases} 0 & i < 0 \\ 1 & i \geq 0. \end{cases} \end{cases} \quad (9.5)$$

with the cubic bistability (1.2) with fixed  $a = .72$ .

In particular, as we increase the diffusion parameter  $d$  we expect the wave to go through four phases. This is numerically confirmed by the results in Figs. 10 and 11. Indeed, for  $d > 0$  sufficiently small, the wave is pinned ( $c = 0$ ). As we increase  $d$  the wave moves to the right ( $c > 0$ , or outwards in the circular depiction of  $\mathcal{T}_2$ ), then it is pinned again  $c = 0$  and once the diffusion is sufficiently strong it propagates to the left ( $c < 0$ , or inwards in the circular depiction of  $\mathcal{T}_2$ ). We note that the transition boundaries for  $d$  correspond well with the numerical results from Example 9.1.

**Acknowledgements** HJH and MJ acknowledge support from the Netherlands Organization for Scientific Research (NWO) (grant 639.032.612). PS and VŠ gratefully acknowledge the support by the Czech Science Foundation grant no. GA22-18261S.

## References

- [1] A. Arenas, A. Díaz-Guilera and R. Guimera (2001), Communication in networks with hierarchical branching. *Physical review letters* **86**(14), 3196.
- [2] D. G. Aronson and H. F. Weinberger (1975), Nonlinear diffusion in population genetics, combustion, and nerve pulse propagation. In: *Partial differential equations and related topics*. Springer, pp. 5–49.
- [3] J. Bell (1981), Some threshold results for models of myelinated nerves. *Mathematical Biosciences* **54**(3-4), 181–190.
- [4] J. Bell and C. Cosner (1984), Threshold behavior and propagation for nonlinear differential-difference systems motivated by modeling myelinated axons. *Quart. Appl. Math.* **42**(1), 1–14.
- [5] J. W. Cahn (1960), Theory of Crystal Growth and Interface Motion in Crystalline Materials. *Acta Met.* **8**, 554–562.
- [6] X. Chen, J. S. Guo and C. C. Wu (2008), Traveling Waves in Discrete Periodic Media for Bistable Dynamics. *Arch. Ration. Mech. Anal.* **189**, 189–236.
- [7] S. N. Dorogovtsev and J. F. F. Mendes (2014), *Evolution of Networks: From Biological Nets to the Internet and WWW*. Oxford University Press.
- [8] A. Erdős, P.; Rényi (1959), On random graphs I. *Publ. Math. Debrecen* **6**, 290–297.
- [9] P. C. Fife (2013), *Mathematical aspects of reacting and diffusing systems*, Vol. 28. Springer Science & Business Media.
- [10] P. C. Fife and J. B. McLeod (1977), The approach of solutions of nonlinear diffusion equations to travelling front solutions. *Archive for Rational Mechanics and Analysis* **65**(4), 335–361.
- [11] R. A. Fisher (1937), The wave of advance of advantageous genes. *Annals of eugenics* **7**(4), 355–369.



- [12] A. Hoffman and M. Holzer (2019), Invasion fronts on graphs: The Fisher-KPP equation on homogeneous trees and Erdős-Rényi graphs. *Discrete & Continuous Dynamical Systems - B* **24**(2), 671–694.
- [13] H. J. Hupkes, L. Morelli, W. M. Schouten-Straatman and E. S. Van Vleck (2018), Traveling waves and pattern formation for spatially discrete bistable reaction-diffusion equations. In: *International Conference on Difference Equations and Applications*, Springer. pp. 55–112.
- [14] H. J. Hupkes, L. Morelli, P. Stehlík and V. Švígler (2019), Multichromatic travelling waves for lattice Nagumo equations. *Applied Mathematics and Computation* **361**, 430–452.
- [15] J. P. Keener (1987), Propagation and its failure in coupled systems of discrete excitable cells. *SIAM Journal on Applied Mathematics* **47**(3), 556–572.
- [16] H. Kori and A. S. Mikhailov (2006), Strong effects of network architecture in the entrainment of coupled oscillator systems. *Physical Review E* **74**(6), 066115.
- [17] N. E. Kouvaris, H. Kori and A. S. Mikhailov (2012), Traveling and Pinned Fronts in Bistable Reaction-Diffusion Systems on Networks. *PLoS ONE* **7**(9), e45029.
- [18] J. Mallet-Paret (1999), The Fredholm Alternative for Functional Differential Equations of Mixed Type. *Journal of Dynamics and Differential Equations* **11**(1), 1–47.
- [19] J. Mallet-Paret (1999), The global structure of traveling waves in spatially discrete dynamical systems. *Journal of Dynamics and Differential Equations* **11**(1), 49–127.
- [20] J. Moser (2016), *Stable and random motions in dynamical systems*. Princeton university press.
- [21] J. Nagumo, S. Arimoto and S. Yoshizawa (1962), An active pulse transmission line simulating nerve axon. *Proceedings of the IRE* **50**(10), 2061–2070.
- [22] Y. Nishiura, T. Teramoto and K.-I. Ueda (2003), Scattering and separators in dissipative systems. *Physical Review E* **67**(5), 056210.
- [23] L. A. Ranvier (1878), *Leçons sur l’Histologie du Système Nerveux, par M. L. Ranvier, recueillies par M. Ed. Weber*. F. Savy, Paris.
- [24] F. Sélley, A. Besenyei, I. Z. Kiss and P. L. Simon (2015), Dynamic control of modern, network-based epidemic models. *SIAM J. Appl. Dyn. Syst.* **14**(1), 168–187.
- [25] A. Slavík (2020), Lotka-Volterra competition model on graphs. *SIAM J. Appl. Dyn. Syst.* **19**(2), 725–762.
- [26] P. Stehlík (2017), Exponential number of stationary solutions for Nagumo equations on graphs. *J. Math. Anal. Appl.* **455**(2), 1749–1764.
- [27] R. Van Der Hofstad (2016), *Random Graphs and Complex Networks: Volume 1*, Vol. 43. Cambridge University Press.
- [28] B. Zinner (1992), Existence of traveling wavefront solutions for the discrete Nagumo equation. *J. Differential Equations* **96**(1), 1–27.